Published in final edited form as:

Nature. 2014 November 20; 515(7527): 436–439. doi:10.1038/nature13682.

Transcript RNA-templated DNA recombination and repair

Havva Keskin[1], **Ying Shen**[1,2], **Fei Huang**[3], **Mikir Patel**[3], **Taehwan Yang**[1], **Katie Ashley**[1], **Alexander V. Mazin**[3], and **Francesca Storici**[1,*]

[1]School of Biology, Georgia Institute of Technology, Atlanta, Georgia, 30332, USA.

[3]Department of Biochemistry and Molecular Biology, Drexel University College of Medicine, Philadelphia, Pennsylvania, 19102, USA.

Abstract

Homologous recombination (HR) is a molecular process that plays multiple important roles in DNA metabolism, both for DNA repair and genetic variation in all forms of life[1]. Generally, HR involves exchange of genetic information between two identical or nearly identical DNA molecules[1]; however, HR can also occur between RNA molecules, as shown for RNA viruses[2]. Previous research showed that synthetic RNA oligonucleotides (oligos) can template DNA double-strand break (DSB) repair in yeast and human cells[3,4], and artificial long RNA templates injected in ciliate cells can guide genomic rearrangements[5]. Here we report that endogenous transcript RNA mediates HR with chromosomal DNA in yeast *Saccharomyces cerevisiae*. We developed a system to detect events of HR initiated by transcript RNA following repair of a chromosomal DSB occurring either in a homologous but remote locus (in *trans*), or in the same transcript-generating locus (in *cis*) in reverse transcription defective yeast strains. We found that RNA-DNA recombination is blocked by ribonucleases (RNases) H1 and H2. In the presence of RNases H, DSB repair proceeds through a cDNA intermediate, whereas in their absence, it proceeds directly through RNA. The proximity of the transcript to its chromosomal DNA partner in *cis* facilitates Rad52-driven HR during DSB repair. In accord, we demonstrate that yeast and human Rad52 proteins efficiently catalyze annealing of RNA to a DSB-like DNA end *in vitro*. Our results reveal a novel mechanism of HR and DNA repair templated by transcript RNA. Thus, considering the abundance of RNA transcripts in cells, the impact of RNA on genomic stability and plasticity could be vast.

*Correspondence and request for materials should be addressed to F.S. (storici@gatech.edu).

[2]Present address: Division of Computational Biomedicine Section, Boston University School of Medicine, Boston, Massachusetts, 02118, USA.

Author Contributions H.K. conducted most of the experiments with yeast samples and performed most of the statistical analysis of the data; Y.S. constructed initial yeast strains and performed initial yeast tests with the assistance of K.A. and helped in the data analysis; F.H. and M.P. performed *in vitro* tests with yeast and human Rad52; T.Y. conducted the transposition assay; A.V.M. designed and analyzed *in vitro* experiments; F.S. together with H.K. and Y.S. designed experiments, assisted data analysis and wrote the manuscript with input from A.V.M. and suggestions from all authors.

The authors declare no competing financial interest. Readers are welcome to comment on the online version of the paper.

Supplementary Information is linked to the online version of the paper at www.nature.com/nature.

Online Content Additional Methods and Extended Data display items are available in the online version of the paper; references unique to these sections appear only in the online paper.

Keywords

RNA-DNA recombination; transcript RNA; DSB repair; homologous recombination; RNase H; yeast Rad52; human RAD52; RNA-templated DNA repair; reverse transcription; cDNA; Ty transposition; RNA-DNA heteroduplexes; RNA-DNA hybrids; Aicardi-Goutieres Syndrome; AGS; central dogma of molecular biology

To investigate the capacity of transcript RNA to recombine with genomic DNA, we examined if a chromosomal DSB could be repaired directly by endogenous RNA in yeast *S. cerevisiae* cells. We designed a strategy in which we could induce a DSB in the *HIS3* marker gene and monitor precise repair of the DSB by a homologous transcript messenger RNA by restoration of the *HIS3* function resulting in histidine prototrophic (His^+) cells (see Methods). We developed two experimental yeast cell systems, *trans* and *cis*, in strains YS-289, 290 and YS-291, 292, respectively (Extended Data Table 1). The *trans* system is designed to test the ability of a spliced (intron-less) antisense *his3* transcript from chromosome (Chr) III to repair a DSB in a different *his3* allele on Chr XV, which contains an engineered HO endonuclease cutting site (Fig. 1a and Extended Data Fig. 1a,b). Differently, the *cis* system is designed to test the capacity of the spliced antisense *his3* transcript from Chr III to repair a HO endonuclease-induced DSB located inside the intron of the same *his3* locus (Fig. 1b and Extended Data Fig. 1c). In both the *trans* and *cis* cell systems, the spliced antisense *his3* transcript RNA can serve as a homologous template to repair the broken *his3* DNA and restore its function. However, given the abundance of Ty retrotransposons in yeast cells, the spliced antisense *his3* RNA could potentially be reverse transcribed by the Ty reverse transcriptase (RT) in the cytoplasm within the Ty particles to cDNA that could then recombine with the homologous broken *his3* sequence or be captured by NHEJ at the HO break site to produce His^+ cells[6-8]. To distinguish DSB repair mediated by transcript RNA-template from repair mediated by cDNA-template, we performed the *trans* and *cis* assays in two yeast strains that either contained a wild-type *SPT3* gene or its null allele, which reduces Ty RT function over 100-fold[3,8,9]. In both assays, cells containing wild-type *SPT3* produced numerous His^+ colonies after DSB induction (Fig. 1c and Table 1a). As expected, the frequency of His^+ colonies in the *trans* system was significantly higher than that in the *cis* system because the *his3* transcript is continuously generated in the presence of galactose. In contrast, production of the full *his3* transcript is immediately terminated upon DSB formation in the *cis* system. This frequency difference is not specific to the particular genomic loci in which the DSBs are induced, as transformation by DNA oligos (HIS3.F and HIS3.R) designed to repair the broken *his3* gene produced the same frequency of His^+ colonies in the two systems (Extended Data Tables 2a and 3) demonstrating that the HO DSB stimulates HR in the *trans* and *cis* systems equally well. Notably, almost all the His^+ colonies are dependent on *SPT3* function indicating that the DSB in *his3* is repaired exclusively via the cDNA pathway (Fig. 1c and Table 1a). This finding demonstrates that if an actively transcribed gene is broken, it can be repaired using a cDNA template derived from its intact transcript. Moreover, these data also support the model that reverse transcribed products from any sort of RNA can be a significant source of genome modification at DSB sites[10] (and references therein).

In order for RNA to recombine with DNA, a required intermediate step is likely the formation of an RNA-DNA heteroduplex. We therefore deleted the genes coding for RNase H1 (*RNH1*) and/or the catalytic subunit of RNase H2 (*RNH201*), which both cleave the RNA strand of RNA-DNA hybrids[11]. Remarkably, while deletion of *RNH1* slightly increased the frequency of His^+ colonies in the *trans* system, deletion of *RNH201* increased the frequency of His^+ colonies in both the *trans* and *cis* systems, and combined deletion of *RNH1* and *RNH201* resulted in an even stronger increase of His^+ colonies in both systems. Moreover, we detected His^+ colonies in *rnh1 rnh201* cells in the absence of *SPT3* (Fig. 1c and Table 1a). Interestingly, there were more His^+ colonies in *cis rnh1 rnh201 spt3* than in *trans*, and the frequency of His^+ colonies observed in the *rnh1 rnh201 spt3* relative to *spt3* cells was much higher in *cis* (>69,000) than in *trans* (>6,400) (Fig. 1c and Table 1a). If DSB repair in *rnh1 rnh201 spt3* cells had been due to cDNA, we would have expected a higher His^+ frequency in the *trans* than in the *cis* system, as observed in wild-type cells. The fact that the His^+ frequency is higher in the *cis* system suggests that DSB repair is not mediated by cDNA but rather RNA or predominantly RNA. To further examine the possibility that residual cDNA rather than transcript RNA is responsible for *his3* correction in *cis rnh1 rnh201 spt3* cells, we introduced a *trans* system directly in these cells and in the control *cis* wild-type cells. When wild-type cells of the *cis* system were transformed with a low-copy-number plasmid carrying the *pGAL1-mhis3AI* cassette (BDG606, see Methods), they displayed a large (a factor of 4,000) increase in the His^+ frequency following DSB induction in *his3* compared to the same cells transformed with the control empty vector (BDG283). On the contrary, in *cis rnh1 rnh201 spt3* cells BDG606 did not significantly increase the His^+ frequency (Fig. 1d and Extended Data Table 4). These results argue against the role of residual cDNA in template-dependent DSB repair in *cis rnh1 rnh201 spt3* cells and support a predominant, direct template function of the *cis his3* transcript RNA in these cells. Overall, these data support the conclusion that a transcript RNA can directly repair a DSB in *cis* in *rnh1 rnh201* and *rnh1 rnh201 spt3* cells. The physical proximity of the *his3* transcript to its own *his3* DNA during transcription could facilitate annealing of the broken DNA ends to the transcript. This possibility is consistent with the fact that closer donor sequences repair DSBs more efficiently[12,13] and that mature transcript RNAs are rapidly exported to the cytoplasm or degraded after completion of transcription[14].

To confirm that inactivation of RNase H1 and H2 allows for direct transcript RNA repair of a DSB in homologous DNA, we conducted a complementation test in the *cis* system using a vector expressing either a catalytically inactive mutant of *RNH201, rnh201*-D39A[15], or wild-type *RNH201*. Results showed that when wild-type *RNH201* was expressed from the plasmid in *rnh1 rnh201 spt3* cells, there were no His^+ colonies following DSB induction (Extended Data Fig. 2a). Deletion of *SPT3* is a well-established and robust method to suppress RT and formation of cDNA in yeast[3,8,9]. However, to prove that the increased frequency of His^+ detected in the *cis* relative to the *trans rnh1 rnh201 spt3* background was not solely linked to *SPT3* deletion, we impaired cDNA formation by deleting the *DBR1* gene, which codes for the RNA debranching enzyme Dbr1[16,17], or by using the RT inhibitor foscarnet (phosphonoformic acid, PFA)[18]. Results shown in Fig. 1c and Extended Data Table 5a support our conclusion that RNA transcripts can directly repair a DSB in chromosomal DNA without being first reverse transcribed into cDNA in *rnh1 rnh201* cells.

Efficient generation of His$^+$ colonies in *cis* wild-type, *rnh1 rnh201*, or *rnh1 rnh201 spt3* cells requires transcription and splicing of the antisense *his3* and DSB formation in the *his3* gene. Deletion of *pGAL1* upstream of *his3* on Chr III, deletion of the HO endonuclease gene, or growing cells in glucose medium, in which HO is repressed, drastically decreased His$^+$ frequency (Extended Data Fig. 2b,c and Extended Data Table 5b,c). Similarly, yeast wild-type, *rnh1 rnh201* and *rnh1 rnh201 spt3* cells of the *cis* system containing a 23-bp truncation of the artificial intron in *his3* lacking the 5'-splice site (Extended Data Table 1 and Extended Data Figure 1c) produced no His$^+$ colonies following DSB induction (Fig. 1e and Extended Data Table 5d), yet these cells were efficiently repaired by HIS3.F and HIS3.R synthetic oligos indicating that the DSB occurred in these cells (Extended Data Table 3).

Next, to examine whether DSB repair frequencies at the *his3* locus in *trans* and in *cis* correlate with the expression level of antisense *his3* transcript, we performed quantitative real time PCR (qRT-PCR). The qRT-PCR data showed that with increased time of incubation in galactose medium (from 0.25 to 8 h) the *trans* strains had significantly more *his3* RNA than the *cis* strains in all backgrounds including the *rnh1 rnh201 spt3.* Also the levels of *his3* transcript dropped significantly from 0.25 to 8 h in galactose in *cis* but not in *trans*, except for the *cis* strain in which the *HO* gene was deleted (Extended Data Fig. 2d). These results are expected in the *cis* strains because as soon as the HO DSB is made, a full *his3* transcript cannot be generated. Therefore, these data corroborate the conclusion that the higher frequency of His$^+$ colonies obtained in *cis* than in *trans rnh1 rnh201 spt3* cells (Fig. 1c and Table 1a) is not due to more abundant and/or more stable transcript but rather to the proximity of the transcript to the target DNA.

PCR analysis of 10 random His$^+$ colonies from each of the *trans* and the *cis rnh1 rnh201 spt3* backgrounds, and Southern blot analysis of three samples from each background showed that the *his3* locus that was originally disrupted by the HO site (*trans* background), or by the intron with the HO site (*cis* background), was indeed corrected to intact *HIS3* sequence. No integration of the *HIS3* gene at the HO site or elsewhere in the genome was detected in all tested clones (20/20) excluding possible mechanisms of repair via capture of cDNA by end joining or via transposition (Fig. 2a and Extended Data Figs. 3 and 4a-c). We also excluded that double deletion of *RNH1* and *RNH201* resulted in increased level of Ty transposition. In fact, results presented in Extended Data Table 6 showed transposition rate a factor of 3-14 lower in null *rnh1 rnh201* than in wild-type cells. This could be due to an increase of non-productive Ty RNA-DNA substrates for the Ty integrase, resulting in abortive integrations and/or titration of the enzyme. Sequence analysis of 24 random His$^+$ colonies from the *cis rnh1 rnh201 spt3* background revealed that all 24 clones had the precise sequence as the spliced antisense *his3* transcript and did not present a typical end joining pattern with small in/del/substitution mutations (Extended Data Fig. 1c and Extended Data Table 2b). These results, together with our observation of no His$^+$ colony formation in cells unable to splice the intron in *his3* (Fig. 1e and Extended Data Table 5d), strongly support an HR mechanism of DSB repair by transcript RNA in *cis rnh1 rnh201 spt3* cells.

Previous studies showed the ability of *E. coli* RecA to promote pairing between duplex DNA and single-strand RNA *in vitro*[19,20]. Recent work suggests that Rad51 can promote

formation of RNA-DNA hybrids in yeast[21]. Here, we show that transcript RNA-directed chromosomal DNA repair is stimulated by the function of Rad52 but not Rad51 recombination protein[22]. Rad52 is important for HR both via single-strand annealing (SSA) and via strand invasion[1,22]. DSB repair by transcript RNA was reduced over 14-fold in *cis rnh1 rnh201 spt3 rad52* but was increased by a factor of 4 in *cis rnh1 rnh201 spt3 rad51* compared to *rnh1 rnh201 spt3* cells (Table 1b). Noticeably, our *in vitro* experiments demonstrate that both yeast and human Rad52 efficiently promote annealing of RNA to a DSB-like DNA end (Fig. 2b-d; Extended Data Fig. 4d-h). Importantly, Rad52 catalyzes the reaction with RNA with nearly the same rate as the reaction with ssDNA of the same sequence. Moreover, RPA, a ubiquitous ssDNA binding protein[1], caused in our experiments a moderate inhibition of Rad52-promoted annealing between complementary ssDNA molecules, but not between ssRNA and ssDNA molecules. Thus in the presence of RPA, the annealing between ssRNA and ssDNA proceeded with higher efficiency than the reaction between ssDNA molecules (Fig. 2b-d; Extended Data Fig. 4d-g).

In vivo, cDNA and/or RNA-dependent DSB repair may be especially important in the absence of functional Rad51 that prevents repair by the uncut sister chromatid via strand invasion[23]. Indeed our results show that deletion of *RAD51* increases the frequency of repair by cDNA and/or RNA (Table 1b). Hence, considering the bias observed for DSB repair in *cis vs. trans* when Ty RT was impaired, we propose a model that in the absence of RNase H function, transcript RNA mediates DSB repair preferentially in *cis* via a Rad52-facilitated annealing mechanism. In this mechanism, the transcript may provide a template that either bridges broken DNA ends to facilitate precise re-ligation or initiate SSA via an RT-dependent extension of the broken DNA ends (Fig. 3). The RT activity could likely be contributed by a replicative DNA polymerase[3], minimal Ty RT, or both.

Current view in the field is that RNA-DNA hybrids formed by the annealing of transcript RNA with complementary chromosomal DNA either in *cis* or in *trans* are mainly a cause of DNA breaks, DNA damage and genome instability[24]. Here, we demonstrate that under genotoxic stress transcript RNA are recombinogenic and can efficiently and precisely template DNA repair in the absence of RNase H function in yeast. In the central dogma of molecular biology, the transfer of genetic information from RNA to DNA is considered to be a special condition, which has been restricted to retroelements[25] and telomeres[26]. Our data show that the transfer of genetic information from RNA to DNA occurs with an endogenous generic transcript (*his3* antisense), and is thus a more general phenomenon than previously anticipated. In addition, *in vitro* RNA-DNA annealing was markedly promoted not only by yeast but also human RAD52, suggesting that transcript RNA-templated DNA repair could occur in human cells. RNA transcripts could template DNA damage repair at highly transcribed loci, in cells that do not divide (lack sister chromatids), or have more stable RNA-DNA heteroduplexes, like those defective in RNASEH2 of Aicardi-Goutieres Syndrome (AGS) patients[27]. Our findings lay the groundwork for future exploration of RNA-driven DNA recombination and repair in different cell types.

Methods

Experimental design to explore transcript-RNA templated chromosomal DSB repair in yeast

In the experimental design to explore transcript-RNA templated chromosomal DSB repair it is critical to discriminate repair of the DSB by transcript RNA from repair by the DNA region that generates the transcript. Also translation of the repairing transcript mRNA should not produce the functional His3 protein. Moreover, it is essential that DSB repair would not restore the *HIS3* marker sequence by simple end ligation via NHEJ. To satisfy these requirements, the DNA region that generates the transcript was constructed to contain a *his3* allele on Chr III consisting of a yeast *HIS3* gene interrupted by an artificial intron (*AI*) in the antisense orientation (*mhis3AI* cassette), which was previously utilized to study reverse transcription in yeast[28,29]. The antisense *his3* RNA is not translated into the functional His3 protein. Moreover, after intron splicing, the transcript RNA sequence has no intron, while the DNA region that generates the transcript retains the intron; thus they are distinguishable. We developed two experimental yeast cell systems, *trans* and *cis* (Fig. 1a,b and Extended Data Fig. 1) in strains YS-289, 290 and YS-291, 292, respectively (Extended Data Table 1). In both systems, transcription of the antisense *his3* RNA and expression of the HO nuclease are regulated by the galactose inducible promoter (*pGAL1*). In addition, these yeast cell systems are auxotrophic for histidine (His^-) and thus do not grow on media without histidine. Upon induction of the HO DSB, the broken *his3* allele of the *trans* and *cis* cell systems can, in principle, only be repaired to a functional *HIS3* allele by recombination with a homologous template. Alternative mechanism of *HIS3* repair by ligation of the broken ends via NHEJ is inefficient in this system ($<0.1/10^7$ viable cells) (data not shown), as the *HIS3* gene is disrupted by a long sequence with the HO site (*trans* system) or an intron and the HO site (*cis* system) (Extended Data Fig. 1b,c).

To impair DSB repair by cDNA deriving from the *his3* antisense, we deleted the *SPT3* or the *DBR1* gene. *SPT3* encodes for a subunit of the SAGA and SAGA-like transcriptional regulatory complexes and its null allele reduces Ty RT function over 100-fold[3,8,9]. *DBR1* encodes for the RNA debranching enzyme Dbr1 and its null allele in yeast cells impairs cDNA formation and diminishes Ty transposition up to a factor of 10-fold[16,17]. As further proof that we can detect DSB repair by transcript RNA independently of cDNA, we performed the *trans* and *cis* assays with and without RNase H functions in the presence of foscarnet (phosphonoformic acid, PFA), an inhibitor of the human immunodeficiency virus RT, which blocks Ty reverse transcription in yeast[18] (and data not shown).

Yeast strains

The yeast strains used in this work are listed in Extended Data Table 1 and derive from FRO-767 strain[3], which contains the site for the HO site-specific endonuclease in the middle of the *LEU2* gene on Chr III. A gene cassette carried on plasmid pSM50[28,29] containing the *his3* gene disrupted by an artificial intron (*AI*) and regulated in the antisense orientation by the galactose inducible promoter *pGAL1* and containing the *URA3* marker gene (*pGAL1-mhis3AIURA3*) was integrated into the *leu2* locus of strain FRO-767 after DSB induction at the HO site by the gene collage technique with no PCR amplification[30]. The *URA3* gene

was then replaced with the *ADE3* gene generating strain FRO-1073. To build the strains of the *trans* system, an HO site was integrated into the endogenous *HIS3* locus on Chr XV of FRO-1073 exactly in the same position in which the *AI* was inserted in the *pGAL1-mhis3AI* cassette using the "*delitto perfetto*" method, as previously described[30,31], to generate FRO-1075, 1080. The correct sequence and insertion position of the HO site was confirmed by sequence analysis. For constructing strains of the *cis* system, first the *his3* gene disrupted by the HO site of FRO-1075 and 1080 was replaced with a *TRP1* gene to generate YS-164, 165, and then an HO cutting site was integrated into the intron *AI* in the *his3* cassette on Chr III to generate strains YS-172,174. To be cautious to avoid any possibility of transcription from Ty into the *pGAL1-mhis3AI* cassette in both the *trans* and *cis* systems, the Ty2 element located upstream of the *leu2* locus on Chr III, *YCLWTy2-1*, was deleted following the "*delitto perfetto*" method to generate YS-289, 290 (*trans* system) and YS-291,292 (*cis* system). These new strain constructs were verified by PCR and sequence analysis to confirm correct constructions. However, no difference in the frequency of His^+ cells was observed between the strains with the *YCLWTy2-1* and those without it for the strains of both the *trans* and *cis* systems (data not shown). Deletion mutants for the *trans* YS-289, 290, and the *cis* 291, 292 strains contain either the *kanMX4, hygMX4, natMX4* and/or the *Kluyveromyces lactis URA3* (*KlURA*3) marker gene in place of the open reading frame or the promoter of the gene/s of choice. All gene disruptions were confirmed by colony PCR. Strains HK-396, 400 and HK-391, 394 were constructed using the "*delitto perfetto*" method by deleting the first 23 bp on the 5' end of the *AI* via insertion of the CORE cassette, and then by popping out the CORE cassette with a pair of oligonucleotides. These constructs were confirmed by sequence analysis. Strain HK-404, 407 was obtained by deleting the *SPT3* gene with *kanMX4* from HK-391, 394. The FRO-1092, 1093 strain is *rad52*Δ and has only one *his3* allele, the endogenous one on Chr XV that has been inactivated by the HO site.

Standard genetic, molecular biology techniques and plasmids

Yeast genetic methods and molecular biology analyses were done as described[3,30,31]. The BDG606 vector[32] and the BDG283 control vector (a gift from D. Garfinkel), used to verify a direct role of transcript RNA in DSB repair (Extended Data Table 4), are centromeric plasmids with the *URA3* marker. BDG606 contains the *pGAL1-mhis3AI* cassette and BDG283 contains only *pGAL1.* The plasmids used for the complementation assay with RNase H2 are Yep195SpGAL, which is a 2-micron high-copy expression plasmid containing the *URA3* selectable marker[33], Yep195SpGAL containing the wild-type *RNH201* gene (Yep195SpGAL-*RNH201*) inserted by gap repair, and Yep195SpGAL-*rnh201*-D39A constructed by *in vitro* mutagenesis (Quick Change Mutagenesis Kit, Stratagene, La Jolla, CA) of Yep195SpGAL-*RNH201* and confirmed by sequence analysis. To confirm occurrence of the HO DSB following incubation in the 2% galactose medium, the percentage of G2 arrested cells was determined right before adding galactose and after 8-h incubation in galactose as previously described[34] (Extended Data Fig. 2c). All primers used for strain and plasmid constructions, PCR verifications and sequence analyses are available upon request. Samples for sequencing were submitted to Eurofins MWG Operon (Huntsville, AL). Southern blot experiment was done as follows. Cells from colonies growing on YPD or His^- were grown on YPD O/N. Genomic DNA was extracted as

described[35] and digested with either BamHI or NarI restriction enzyme. After digestion, column purification was applied by using QIAquick PCR Purification Kit (QIAGEN). DNA was run in a 0.8% agarose gel. Following electrophoresis and Southern blotting chromosomal regions containing the *HIS3* gene were detected using a [α-32P]ATP (PerkinElmer) labeled (Prime-It RmT Random Primer Labelling Kit, Agilent Technologies) 250-bp *HIS3*-specific probe. Membrane was exposed to a phosphor screen for 3 days. Images were taken with Typhoon Trio$^+$ (GE Healthcare) and obtained with ImageQuant (GE Healthcare).

Trans and *cis* assays using patches or liquid cultures

Yeast cells of the chosen strains were patched on the rich medium containing yeast extract, peptone and 2% (w/v) dextrose (YPD) and grown at 30 °C for 1 day. The cells were then replica-plated on medium containing yeast extract, peptone and 2% (w/v) galactose (YPGal) or YPGal containing phosphonoformic acid, PFA (2.5 mg/ml) to turn on transcription of the *his3* antisense on Chr III and expression of the HO endonuclease. As a control, cells were also replica-plated from the YPD medium on synthetic complete medium plates lacking histidine (SC-His$^-$) and grown for 3 days at 30 °C. We never detected a single His$^+$ colony from any of the *trans* and *cis* strains used in this study following replica-plating from the YPD medium on SC-His$^-$ (not shown). After 2 days incubation on YPGal medium, these cells were replica-plated on SC-His$^-$ and grown for 3 days at 30 °C to form visible colonies. At this stage, plates were photographed and photo files stored. For experiments using the BDG606 and BDG283 plasmids, cells were replica-plated from SC-Ura$^-$ on SC-Ura$^-$Gal medium, and were then replica-plated on SC-Ura$^-$His$^-$. As a control, cells were also replica-plated from the SC-Ura$^-$ medium SC- Ura$^-$His$^-$ and grown for 3 days at 30 °C.

For the experiments in liquid culture, flasks with 50 ml of liquid medium containing yeast extract, peptone and 2.7% (v/v) lactic acid (YPLac) were inoculated with yeast cells of the chosen strains and incubated in a 30 °C shaker for 24 h. The density of the cultures was determined by counting cells using a hemocytometer and counting under a microscope. Generally, 10^7 or, in rare cases, 10^8 cells (we note that survival is very low on galactose medium) were then plated on YPGal medium, or YPGal medium containing PFA (2.5 mg/ml) for experiments using PFA to obtain from 1 to ~500 His$^+$ colonies per plate after the replica-plating on His$^-$ medium, and grown for 2 days at 30 °C. Two aliquots of 10^4 cells were plated each on one YPGal medium plate, or YPGal medium containing PFA (2.5 mg/ml) for experiments using PFA plate, to measure the cell survival after galactose treatment. After 2 days incubation on YPGal medium, cells were replica-plated on His$^-$ plates and grown for 3 days at 30 °C. The frequency of DSB repair was calculated by dividing the number of His$^+$ colonies on SC-His$^-$ medium by the number of colonies on YPGal medium. The survival was calculated by dividing the number of colonies on YPGal medium by the number of cells plated on the same medium. For experiments using the BDG606 and BDG283 plasmids, cells were treated as described above except that they were plated from YPLac on SC-Ura$^-$Gal medium in different dilutions, and were then replica-plated on SC-Ura$^-$His$^-$. The frequency of His$^+$ colonies was calculated by dividing the number of His$^+$ colonies on SC-Ura$^-$His$^-$ medium by the number of colonies on SC-

Ura⁻Gal medium. The survival was calculated by dividing the number of colonies on SC-Ura⁻Gal medium by the number of cells plated on the same medium.

Oligo Transformation

Transformation by oligos (1 nmol) was performed as described[3]. Induction of the HO DSB was done by incubating cells in 2 % galactose medium for 3 h.

Transposition Assay

Yeast cells of the chosen strains transformed with BDG102 (empty plasmid) or BDG598 (*pGTy-H3mHIS3AI*) plasmid[36] (containing a Ty transposon fused to the *his3* gene, which is in the antisense orientation and disrupted by an artificial intron (*AI*); both Ty and the *his3* antisense are regulated by the galactose inducible promoter) were patched on synthetic complete medium lacking uracil (SC-Ura⁻) and grown overnight at 30 °C. Cells were then replica-plated on synthetic medium lacking uracil with 2% (w/v) galactose (SC-Ura⁻Gal) and grown for 48 or 96 hours at 30 °C or 22 °C, respectively. As control, cells were also replica-plated on SC-His⁻ to determine the background of His^+ clones. After the incubation in galactose, cells were replica-plated on SC-His⁻ and grown for 3 days at 30 °C to form visible colonies. At this stage, plates were photographed and photo files stored. For the experiments in liquid culture, strains with BDG102 or BDG598 were grown in 5 ml SC-Ura⁻ liquid medium or in 10 ml of YPLac liquid medium in a 30 °C shaker for 24 h. Then, 1×10^6 cells were transferred from the SC-Ura⁻ liquid medium into 5 ml SC-Ura⁻ or 5 ml SC-Ura⁻Gal liquid medium and incubated for 48 or 96 h at 30 °C or 22 °C, respectively. After 24 h, YPLac cultures were split in half. One half was kept growing for additional 48 h at 30 °C, while galactose was directly added to the other half to reach 2% and cells were then incubated for 48 h at 30 °C. From glucose and YPLac cultures grown at 22 °C or 30 °C, 10^7 or 10^8 cells were plated on SC-His⁻Ura⁻ medium, respectively, and were grown for 2 days at 30 °C. From galactose cultures grown at 22 °C or 30 °C, 10^5 or 10^6 cells were plated on SC-His⁻Ura⁻ medium, respectively, and were grown for 2 days at 30 °C. Two aliquots of 5×10^2 cells were plated each on one SC-Ura⁻ medium plate, to measure the cell survival after glucose, YPLac or galactose treatment. The rate of formation of His^+ cells was calculated by the maximum-likelihood method of Lea and Coulson[37].

Quantitative real time PCR

RNA was isolated from the chosen yeast strains of the *trans* and *cis* systems using a protocol adapted from a method described previously by Fasken *et al.*[38]. RNA was converted in to cDNA using QuantiTect Reverse Transcription Kit (QIAGEN). SYBER Green qPCR Mix (BioRad) was used for analyzing RNA expression in 96 well plates (Applied Biosystem). The total volume in each well was 20 µl, which consisted of 10 µl of SYBR Green qPCR Mix, 4 µl of nuclease-free water, 2 µl of primers, and 4 µl of cDNA. The cDNA levels were determined using an ABI Prism 7000 RT-PCR machine (Applied Biosystems). ACT1.F and ACT1.R, HIS3.F2 and HIS3.R2 primers were used in this study (Extended Data Table 2a). ACT1 primers were used for normalization. Values for each sample were normalized with ACT1, and then a second normalization was performed by subtracting normalized values of each time point from the control normalized value per each gene[39]. As negative control, CEN16.F and CEN16.R primers were used to show that there is no or minimal qRT-PCR

product derived from a chromosomal region that is not transcribed (Aziz El Hage, personal communication) (data not shown).

Rad52 *in vitro* annealing assay

In vitro assays using yeast or human Rad52 were performed as described[40,41] (and references therein), with all DNA and RNA concentrations expressed in moles of molecules. All oligo sequences are shown in Extended Data Table 2a. A single nucleotide mismatch was incorporated into the dsDNA (relative to ssDNA or RNA) to reduce the spontaneous Rad52-independent annealing. Tailed dsDNA (#508/#509) (0.4 nM) was incubated in the absence or presence of yeast or human RPA (2 nM) in a buffer containing 25 mM Tris acetate, pH 7.5, 100 μg/ml BSA, and 1 mM DTT for 5 min at 37 °C, then yeast or human RAD52 (1.35 nM), respectively, was added and incubation continued for 10 min. Annealing reactions were initiated by adding ^{32}P-labeled ssRNA (#501) or ssDNA (#211) (0.3 nM). Aliquots were withdrawn at indicated time points and deproteinized by incubating samples in stop solution containing 1.5% SDS, 1.4 mg/ml proteinase K, 7% glycerol and 0.1% bromophenol blue for 15 min at 37 °C. Samples were analyzed by electrophoresis in 10% (17:1 acrylamide:bisacrylamide) polyacrylamide gels in 1 X TBE (90 mM Tris-borate, pH 8.0, 2 mM EDTA) at 150 V for 1 h and were quantified using a Storm 840 Phosphorimager and ImageQuant 5.2 software (GE Healthcare).

Data presentation and statistics

Graphs were made using GraphPad Prism 5 (Graphpad Software, La Jolla, CA). The results are each expressed as a median and 95% confidence limits (in parentheses), or alternatively the range when number of repeated experiments was <6. Statistical significant differences between the His^+ frequencies were calculated using the nonparametric two-tailed Mann-Whitney U test[42]. All P values obtained using the Mann-Whitney U test were then adjusted by applying the false discovery rate (FDR) method to correct for multiple hypothesis testing[43] (Supplementary Table 1).

Extended Data

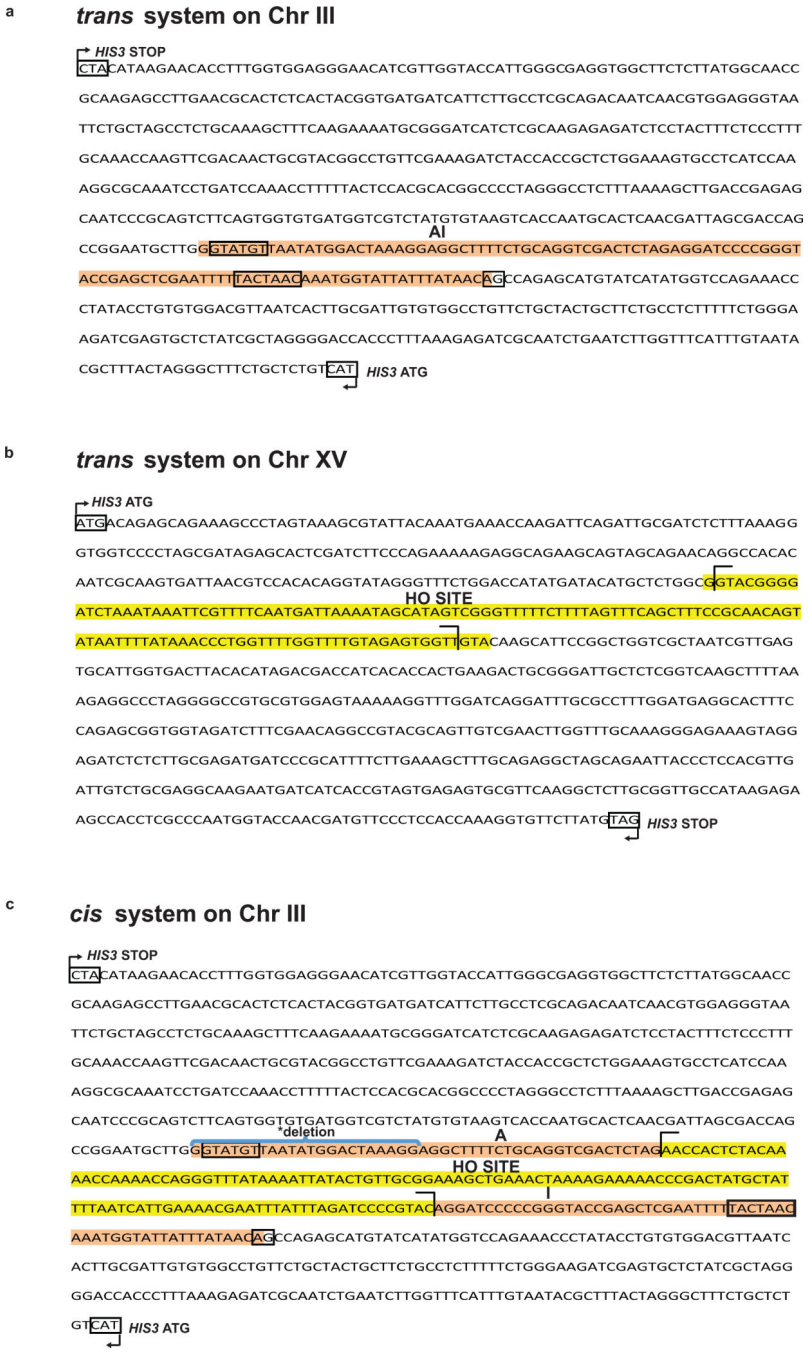

Extended Data Figure 1. DNA sequence of the *his3* loci in the *trans* and *cis* systems

a, *Trans* system on Chr III. *HIS3* ATG and STOP codons are boxed. The *HIS3* gene is disrupted by an insert (orange) carrying the artificial intron (AI). The consensus sequences of the AI are boxed. **b**, *Trans* system on Chr XV. *HIS3* ATG and STOP codons are shown. The *HIS3* gene is disrupted by an insert (yellow) containing the 124-bp HO site (marked by lines). **c**, *Cis* system on Chr III. *HIS3* ATG and STOP codons are shown. The *HIS3* gene is disrupted by an insert (orange) carrying the AI, which contains the 124-bp of the HO site

(yellow and marked by lines). The consensus sequences of the AI are boxed. * indicates a 23-bp deletion of the AI, including the 5'-splice site, made in some strains.

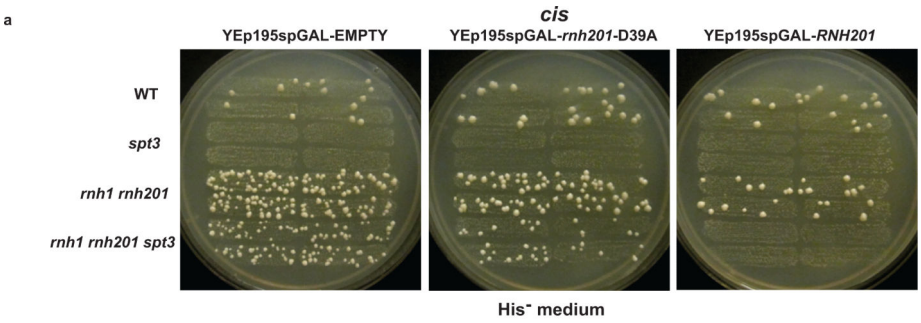

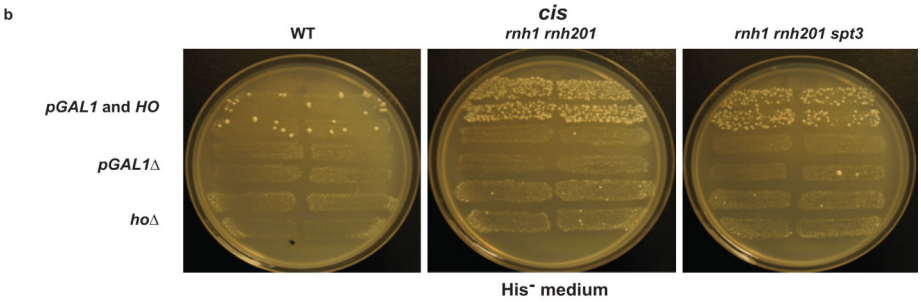

c

cis	0 h GAL			8 h GAL		
Genotype	G1	S	G2	G1	S	G2
WT	75	13	12	24	11	65
rnh1 rnh201	74	14	12	23	11	66
rnh1 rnh201 spt3	66	5	29	35	7	58
pGAL1Δ	83	7	10	27	7	66
rnh1 rnh201 pGAL1Δ	79	6	15	31	6	63
rnh1 rnh201 spt3 pGAL1Δ	73	5	22	28	7	65
hoΔ	90	5	5	69	14	16
rnh1 rnh201 hoΔ	91	4	5	66	19	15
rnh1 rnh201 spt3 hoΔ	70	9	21	59	14	27

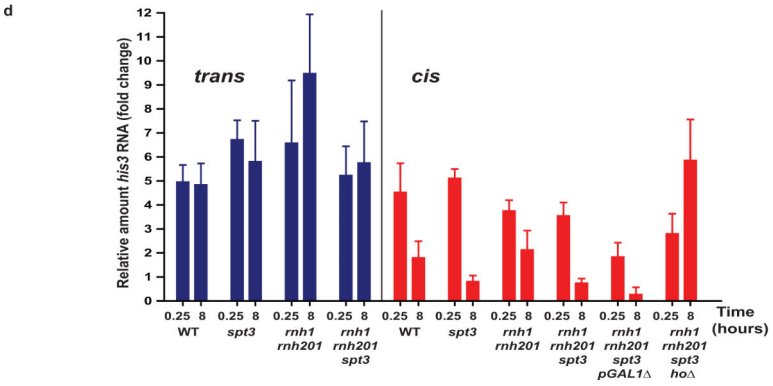

Extended Data Figure 2. Efficient transcript RNA-directed gene modification is inhibited by *RNH201*, requires transcription of the template RNA and formation of a DSB in the target gene

a, Complementation of *rnh201* defect suppresses transcript RNA-templated DSB *repair* in *cis rnh1 rnh201 spt3* cells. WT, *spt3, rnh1 rnh201, rnh1 rnh201 spt3* strains of the *cis* system were transformed by a control empty vector (YEp195spGAL-EMPTY), a vector expressing catalytically inactive (YEp195spGAL-*rnh201*-D39A) or a wild-type form of RNase H2

(YEp195spGAL-*RNH201*). All the vectors have the galactose inducible promoter. Shown is an example of replica-plating results (n = 6) from galactose medium to histidine dropout for the indicated strains and plasmids. **b**, Example of replica-plating results (n = 6) from galactose medium to histidine dropout for the indicated strains of the *cis* system, which have functional *pGAL1* and *HO* gene, or have deleted *pGAL1*, or deleted *HO* gene. **c**, Table with percentages of cells in the G1, S or G2 stage of the cell cycle out of random 200 cells counted for the indicated strains of the *cis* system after 0 h and 8 h from galactose induction. If an HO DSB is made in *his3*, yeast cells arrest in G2, thus, high percentage of G2 arrested cells indicates occurrence of the HO DSB. We also note that strains with *spt3* mutation have higher percentage of G2 cells than strains with wild-type *SPT3* before DSB induction (0 h GAL). **d**, Results of qRT-PCR of *his3* RNA. Cells were grown in YPLac liquid medium O/N, and were collected and prepared for qRT-PCR at 0, 0.25 or 8 h after adding galactose to the medium. *Trans* strains have blue bars, *cis* red, respectively. Data are represented as a fold change value with respect to mRNA expression at time zero, as median with range of 6-8 repeats. The significance of comparisons between fold changes obtained at 0.25 h *vs.* those obtained at 8 h, fold changes of different strains of the *trans* and *cis* system, and between fold changes obtained in the *trans vs. cis* system for the same strains at the same time point was calculated using the Mann-Whitney U test and P values are presented in Supplementary Table 1jI, II and III, respectively.

We note that an apparent higher level of *his3* RNA is detected at 8 h in galactose in both *trans* and *cis rnh1 rnh201* cells relative to the other tested genetic backgrounds. Our interpretation of these results is that *his3* RNA could be more stable in *rnh1 rnh201* cells if present in the form of RNA-DNA heteroduplexes, and this may explain the increased frequency of His^+ colonies observed in both *trans* and *cis* in the *rnh1 rnh201* cells (Fig. 1c and Table 1a).

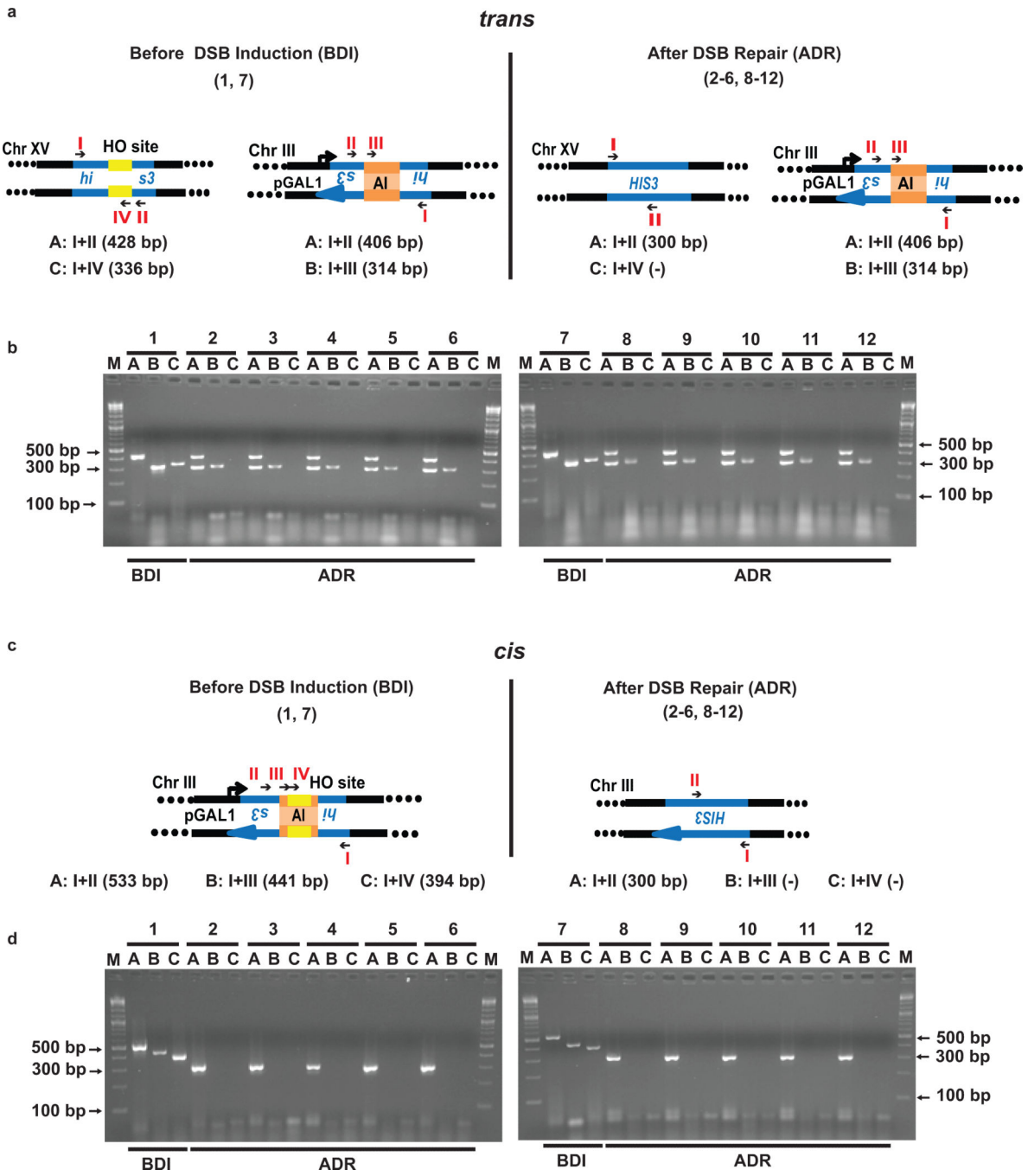

Extended Data Figure 3. Verification of *his3* repair in *trans* and *cis rnh1 rnh201 spt3* cells via an HR mechanism using colony PCR

a, Scheme of the *trans* system before DSB induction (BDI, groups of lanes 1 and 7) and after DSB repair (ADR, groups of lanes 2-6 and 8-12) with the primers used in colony PCR shown as small black arrows and named with roman numerals: I, HIS3.5; II, HIS3.2; III, INTRON.F; IV, HO.F. The primer pairs used for colony PCR are named A (I+II), B (I+III), and C (I+IV), and base-pair sizes of the expected PCR products are shown in parentheses. **b**, Photos of agarose gels with results of colony PCR reactions. M, 2-Log DNA Ladder marker;

the 100, 300 and 500-bp band sizes are pointed by arrows. Groups of lanes 1 and 7, two isolates of *trans rnh1 rnh201 spt3* mutants BDI, each tested with primer pairs A, B and C. Groups of lanes 2-6 and 8-12, ten isolates of *trans rnh1 rnh201 spt3* mutants ADR, each tested with primer pairs A, B and C. **c**, Scheme of the *cis* system before DSB induction (BDI, groups of lanes 1 and 7) and after DSB repair (ADR, groups of lanes 2-6 and 8-12) with the primers used in colony PCR shown as small black arrows and named with roman numerals: I, HIS3.5; II, HIS3.2; III, INTRON.F; IV, HO.F. The primer pairs used for colony PCR are named A (I+II), B (I+III), and C (I+IV), and base-pair sizes of the expected PCR products are shown in parentheses. **d**, Photos of agarose gels with results of colony PCR reactions. M, 2-Log DNA Ladder marker; the 100, 300 and 500-bp band sizes are pointed by arrows. Groups of lanes 1 and 7, two isolates of *cis rnh1 rnh201 spt3* mutants BDI, each tested with primer pairs A, B and C. Groups of lanes 2-6 and 8-12, ten isolates of *cis rnh1 rnh201 spt3* mutants ADR, each tested with primer pairs A, B and C.

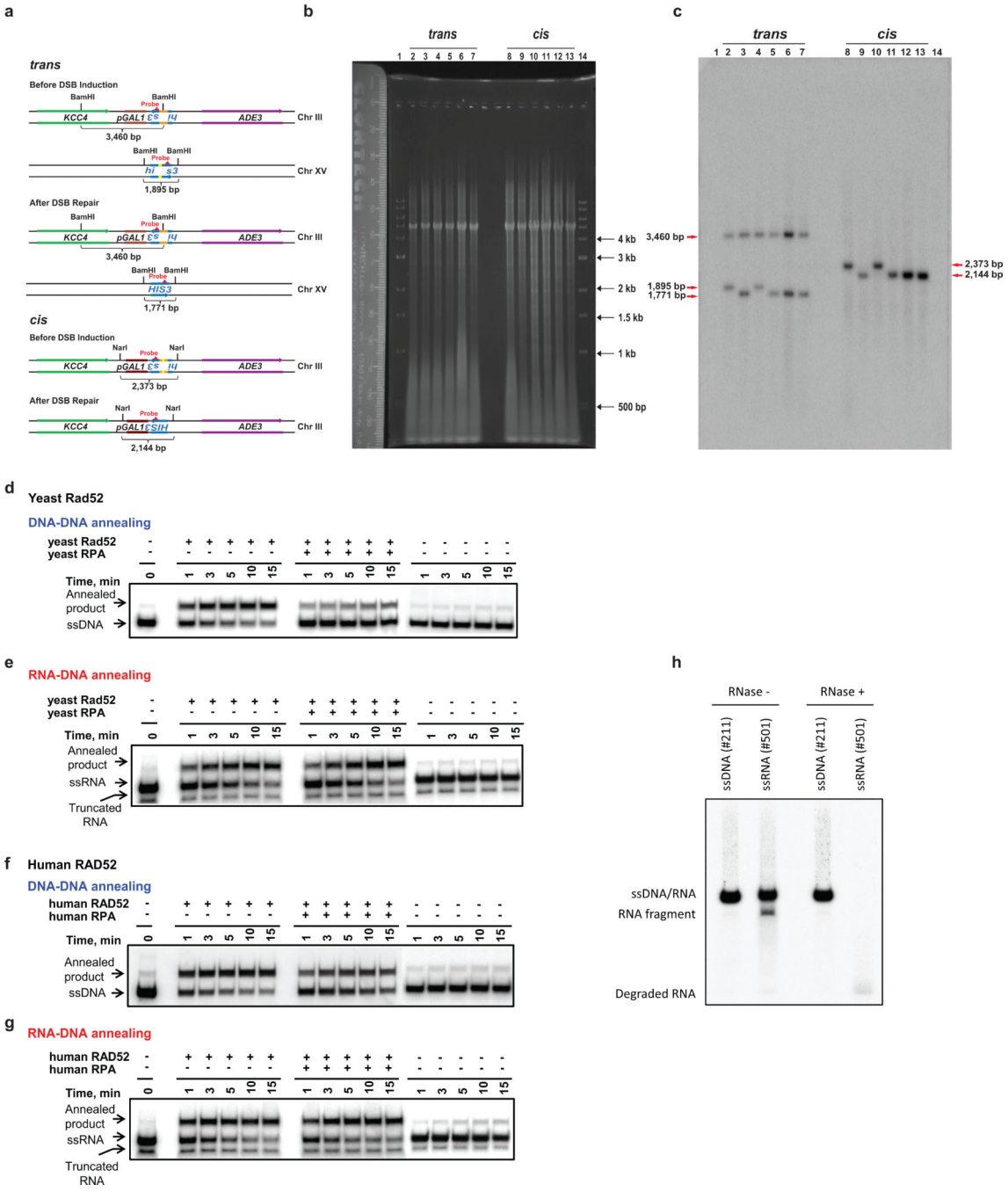

Extended Data Figure 4. RNA-templated DNA repair occurs via HR and requires Rad52

a, Scheme of the *trans* and *cis his3/HIS3* loci in His$^-$ (Before DSB Induction) and His$^+$ (After DSB Repair) cells. The size of the BamHI *(trans)* or NarI *(cis)* restriction digestion products and the position of the *HIS3* probe are shown. **b**, Photo of ruler next to ethidium bromide-stained agarose gel with marker and genomic DNA samples visible before Southern blot. Lanes 1 and 14, 1 kb DNA Ladder; 500 bp, 1 kb, 1.5 kb, 2 kb, 3 kb and 4 kb bands are pointed by arrows. *Trans* WT His$^-$ (lane 2) or His$^+$ (lane 3), *rnh1 rnh201 spt3* His$^-$ (lane 4) or His$^+$ (lanes 5-7) cells, digested with BamHI restriction enzyme. *Cis* WT His$^-$ (lane 8) or

His$^+$ (lane 9), *rnh1 rnh201 spt3* His$^-$ (lane 10) or His$^+$ (lanes 11-13) cells, digested with NarI restriction enzyme. **c**, Southern blot analysis (same as in Fig. 2a, but displaying the entire picture of the exposed membrane) of yeast genomic DNA derived from *trans* WT His$^-$ (lane 2) or His$^+$ (lane 3), *rnh1 rnh201 spt3* His$^-$ (lane 4) or His$^+$ (lanes 5-7) cells, digested with BamHI restriction enzyme and hybridized with the *HIS3* probe, or derived from *cis* WT His$^-$ (lane 8) or His$^+$ (lane 9), *rnh1 rnh201 spt3* His$^-$ (lane 10) or His$^+$ (lanes 11-13) cells, digested with NarI restriction enzyme and hybridized with the *HIS3* probe. Lanes 1 and 14, 1 kb DNA ladder visible in the ethidium bromide-stained gel (panel b). Size of digested DNA bands is indicated by red arrows. The annealing reactions were promoted by either yeast (**d,e**) Rad52 or human (**f,g**) RAD52 (1.35 nM) in the presence or absence of yeast or human RPA, respectively (2 nM). In control protein-free reactions, protein dilution buffers were added instead of the respective proteins. To initiate the annealing reactions, 0.3 nM (molecules) ^{32}P-labeled ssDNA (#211) or ssRNA (#501) were added. The reactions were carried out for the indicated periods of time, and the products of annealing reactions were deproteinized and analyzed by electrophoresis in 10% polyacrylamide gels in 1 X TBE at 150 V for 1 h. Visualization and quantification was accomplished using a Storm 840 Phosphorimager. **e**,Treatment of RNA and DNA oligos with RNase. 3 μM ssDNA (#211) or RNA (#501) was incubated with 100 μg/ml (or 7 U/ml) RNase (QIAgen) in buffer containing 50 mM Hepes, pH 7.5 for 30 min at 37 °C, then 7% glycerol and 0.1% bromophenol blue were added to the samples and incubation continued for another 15 min at 37 °C before they were analyzed by electrophoresis in a 10% (17:1 acrylamide:bisacrylamide) polyacrylamide gel at 150 V for 1 h in 1 X TBE buffer. The gel was quantified using a Storm 840 Phosphorimager. The RNA oligo is completely degraded by RNase but not the DNA oligo.

Extended Data Table 1

Yeast strains used in this study

S. cerevisiae strains used in this study. Strains specifically used for the *trans* or *cis* assay are indicated.

Strain	Relevant genotype	Source
FRO-767	*ho*Δ *hml*Δ::*ADE1 mata*Δ::*hisG hmr*Δ::*ADE1 ade1 leu2*::*HOcs lys5 trp1*::*hisG ura3-52 ade3*::*GAL*::*HO*	[3]
FRO-1072	*ho*Δ *hml*Δ::*ADE1* Δ*mata*::*hisG hmr*Δ::*ADE1 ade1 leu2*::*pGAL1-mhis3AI-URA3 lys5 trp1*::*hisG ura3-52 ade3*::*GAL*::*HO*	this study
FRO-1073	*ho*Δ *hml*Δ::*ADE1 mata*Δ::*hisG hmr*Δ::*ADE1 ade1 leu2*::*pGAL1mhis3AI-ADE3 lys5 trp1*::*hisG ura3-52 ade3*::*GAL*::*HO*	this study
FRO-1074	FRO-1073 *his3*::CORE-UH	this study
FRO-1075,1080 (*trans*)	FRO-1073 *his3*::*HOcs*	this study
FRO-1092, 1093	*ho*Δ *hml*Δ::*ADE1 mata*Δ::*hisG hmr*Δ::*ADE1 ade1 leu2*::*pGAL1-ADE3 lys5 trp1*::*hisG ura3-52 ade3*::*GAL*::*HO his3*::*HOcs rad52*Δ::*kanMX4*	this study
YS-164, 165	FRO-1075, 1080 (*HIS3*::*HOcs*)::*TRP1*	this study
YS-166, 167	YS-164, 165 *pGAL1-mhis3AI*::CORE	this study
YS-172, 174 (*cis*)	YS-166, 167 *pGAL1-mhis3AI*::*HO*	this study
YS-275, 276	FRO-1075, 1080, *YCLWTy2-1*::CORE	this study
YS-278, 281	YS-172, 174 *YCLWTy2-1*::CORE	this study
YS-289, 290 (*trans*) WT	YS-275, 276 *YCLWTy2-1*Δ	this study
YS-291, 292 (*cis*) WT	YS-278, 281 *YCLWTy2-1*Δ	this study
YS-414, 415 (*trans*)	YS-289, 290 *mh1*Δ::*kanMX4*	this study
YS-416, 417 (*cis*)	YS-291, 292 *mh1*Δ::*kanMX4*	this study
YS-410, 411 (*trans*)	YS-289, 290 *mh201*Δ::*hygMX4*	this study
YS-412, 413 (*cis*)	YS-291, 292 *mh201*Δ::*hygMX4*	this study
YS-428, 429 (*trans*)	YS-289, 290 *spt3*Δ::*kanMX4*	this study
YS-440, 441 (*cis*)	YS-291, 292 *spt3*Δ::*kanMX4*	this study
YS-444, 445 (*cis*)	YS-291, 292 *rad52*Δ::*kanMX4*	this study
YS-446, 447 (*cis*)	YS-291, 292 *rad51*Δ::*kanMX4*	this study
HK-76, 77 (*trans*)	YS-289, 290 *dbr1*Δ::*kanMX4*	this study
HK-72, 73 (*cis*)	YS-291, 292 *dbr1*Δ::*kanMX4*	this study
YS-520, 521 (*trans*)	YS-414, 415 *spt3*Δ::*hygMX4*	this study
YS-522, 524 (*cis*)	YS-416, 417 *spt3*Δ::*hygMX4*	this study
YS-452, 453 *(trans)*	YS-410, 411 *spt3*Δ::*hygMX4*	this study
YS-464, 465 (*cis*)	YS-412, 413 *spt3*Δ::*hygMX4*	this study

Strain	Relevant genotype	Source
YS-422, 423 (*trans*)	YS-289, 290 *rnh1*Δ::*NAT rnh201*Δ::*hygMX4*	this study
YS-424, 426 (*cis*)	YS-291, 292 *rnh1*Δ::*NAT rnh201*Δ:: *hygMX4*	this study
YS-476, 477 (*trans*)	YS-289, 290 *rnh1*Δ::*NAT rnh201*Δ::*hygMX4 spt3*Δ::*kanMX4*	this study
YS-486, 487 (*cis*)	YS-291, 292 *rnh1*Δ::*NAT rnh201*Δ::*hygMX4 spt3*Δ::*kanMX4*	this study
YS-490, 491 (*cis*)	YS-424, 426 *rad52*Δ::*kanMX4*	this study
YS-492, 493 (*cis*)	YS-424, 426 *rad51*Δ::*kanMX4*	this study
HK-78, 79 (*trans*)	YS-422, 423 *dbr1*Δ::*kanMX4*	this study
HK-74, 75 (*cis*)	YS-424, 426 *dbr1*Δ::*kanMX4*	this study
HK-213, 215 (*trans*)	YS-422, 423 *dbr1*Δ::*KIURA3*	this study
HK-217, 219 (*cis*)	YS-424, 426 *dbr1*Δ::*KIURA3*	this study
HK-136, 137 (*trans*)	YS-422, 423 *spt3*Δ::*KIURA3*	this study
HK-138, 139 (*cis*)	YS-424, 426 *spt3*Δ::*KIURA3*	this study
HK-194, 197 (*cis*)	HK-138, 139 *rad52*Δ::*kanMX4*	this study
HK-180, 184 (*cis*)	HK-138, 139 *rad51*Δ::*kanMX4*	this study
HK-112, 113 (*trans*)	HK-78, 79 *spt3*Δ::*KIURA3*	this study
HK-110, 111 (*cis*)	HK-74, 75 *spt3*Δ::*KIURA3*	this study
YS-526, 527 (*cis*)	YS-291 *pGAL1*Δ::*KIURA3*	this study
YS-528, 529 (*cis*)	YS-424, 426 *pGAL1*Δ::*KIURA3*	this study
YS-530, 531 (*cis*)	YS-486, 487 *pGAL1*Δ::*KIURA3*	this study
YS-532, 533 (*cis*)	YS-291, 292 *ade3*::*GAL*::*ho*Δ::*KIURA3*	this study
YS-534, 535 (*cis*)	YS-424, 426 *ade3*::*GAL*::*ho*Δ::*KIURA3*	this study
YS-536, 537 (*cis*)	YS-486, 487 *ade3*::*GAL*::*ho*Δ::*KIURA3*	this study
HK-9, 10 (*cis*)	YS-291, 292 + Yep195spGAL	this study
HK-11, 12 (*cis*)	YS-291, 292 + Yep195spGAL-*RNH201*-WT	this study
HK-13, 14 (*cis*)	YS-291, 292 + Yep195spGAL-*mh201*-D39A	this study
HK-15, 16 (*cis*)	YS-440, 441 + Yep195spGAL	this study
HK-17, 18 (*cis*)	YS-440, 441 + Yep195spGAL-*RNH201*-WT	this study
HK-19, 20 (*cis*)	YS-440, 441 + Yep195spGAL-*rnh201*-D39A	this study
HK-21, 22 (*cis*)	YS-424, 426 + Yep195spGAL	this study
HK-23, 24 (*cis*)	YS-424, 426 + Yep195spGAL-*RNH201*-WT	this study
HK-25, 26 (*cis*)	YS-424, 426 + Yep195spGAL-*rnh20*- D39A	this study

Strain	Relevant genotype	Source
HK-27, 28 (*cis*)	YS-486, 487 + Yep195spGAL	this study
HK-29, 30 (*cis*)	YS-486, 487 + Yep195spGAL-*RNH201*-WT	this study
HK-31, 32 (*cis*)	YS-486, 487 + Yep195spGAL-*rnh201*-D39A	this study
YS-301	*MATα his3*Δ1 *leu2*Δ0 *lys2*Δ0 *ura3*Δ0 *trp5*(ΔCC1001-2; G1017→A)	[44]
YS-305	YS-301 *rnh201*Δ::*kanMX4*	[44]
KK-72	YS-305 *rnh1*Δ::*hygMX4*	this study
TY-32, 52	YS-301 + BDG102 (empty vector)	this study
TY-17, 53	YS-301 + BDG598 (*pGTy-H3mHIS3AI*)	this study
TY-36, 66	KK-72 + BDG102 (empty vector)	this study
TY-22, 67	KK-72 + BDG598 (*pGTy-H3mHIS3AI*)	this study
HK-386, 388 (*cis*)	YS-291, 292 *mhis3AI*::CORE	this study
HK-382, 384 (*cis*)	YS-424, 426 *mhis3AI*::CORE	this study
HK-396, 400 (*cis*)	HK-386, 388 *AI*Δ23	this study
HK-391, 394 (*cis*)	HK-382, 384 *AI*Δ23	this study
HK-404, 407 (*cis*)	HK-391, 394 *spt3*Δ::*kanMX4*	this study

Extended Data Table 2

Oligos used in this study and sequence patterns of the *HIS3* region repaired by transcript RNA or via NHEJ

a, Name, size and sequence of the oligos used in this study are described. The specific experiments in which the oligos were utilized are indicated. **b,** Sequence patterns of the *HIS3* region repaired by transcript RNA or via NHEJ. All 24 His^+ *cis rnh1 rnh201 spt3* clones that were sequenced had perfect match with wild-type *HIS3* sequence. Differently, when we examined the sequence of the rare His^+ clones that we could obtain (~$10/10^7$ viable cells) from a strain that had the HO site in *his3* on Chr XV (the construct is identical to that described in Extended Data Fig. 1b) and was *rad52* null (FRO-1092, 1093), 29 out of 29 His^+ samples had replaced 4 nucleotides (TGGC) of *his3* next to the HO site with new sequence. Differences from the WT *HIS3* gene are in bold. A-C, patterns of the *HIS3* region from spontaneous His^+ revertants. Among the 29 sequenced *HIS3* regions, 25 displayed pattern A, 3 displayed pattern B, and 1 displayed pattern C. The four bases inconsistent with the WT *HIS3* affected two codons, causing a silent mutation (GCC → GCG: Ala → Ala) and a missense mutation (AAG → GTA, GTC or GTG: Lys → Val).

a

Name	Size	Sequence	Experiment
HIS3.F	80	5'ACCAATGCACTCAACGATTAGCGACCAGCCGGAATGCTTGGCCAGAGCATGTATCATATGGTCCAGAAACCCTATACCTG	Transformation
HIS3.R	80	5'CAGGTATAGGGTTTCTGGACCATATGATACATGCTCTGGCCAAGCATTCCGGCTGGTCGCTAATCGTTGAGTGCATTGGT	Transformation
His3.F2	20	5' CCTGTTCTGCTACTGCTTCT	qRT-PCR
His3.R2	20	5' CGATCTCTTTAAAGGGTGGT	qRT-PCR
ACT1.F	20	5' TTGGATTCCGGTGATGGTGT	qRT-PCR
ACT1.R	20	5' CGGCCAAATCGATTCTCAAA	qRT-PCR
CEN16.F	20	5' TGAGCAAACAATTTGAACAG	qRT-PCR
CEN16.R	18	5' CCGATTTCGCTTTAGAAC	qRT-PCR
His3.2	20	5' GAGAGCAATCCCGCAGTCTT	Colony PCR
His3.5	20	5' ATGACAGAGCAGAAAGCCCT	Colony PCR
HO.F	20	5' AACCACTCTACAAAACCAAA	Colony PCR
INTRON.F	20	5' GTATGTTAATATGGACTAAA	Colony PCR
S3.1	20	5' TTAAAGAGGCCCTAGGGGCC	Southern blot
S3.2	20	5' CTACATAAGAACACCTTTGG	Southern blot
S3.3	20	5' TTTGCGCCTTTGGATGAGGC	Southern blot
S3.4	20	5' TTGGGCGAGGTGGCTTCTCT	Southern blot
211	48	5' GAAGCATTTATCAGGGTTATTGTCTCATGAGCGGATACATATTTGAAT	Rad52 Annealing
501	48	5' GAAGCAUUUAUCAGGGUUAUUGUCUCAUGAGCGGAUACAUAUUUGAAU	Rad52 Annealing
508	53	5' ATTCAA ATATGTATCCGCTAATGAGACAATAACCCTGATAAATGCTTCACTAG	Rad52 Annealing

a

Name	Size	Sequence	Experiment
509	32	5’ TTATTGTCTCATTAGCGGATACATATTTGAAT	Rad52 Annealing

b

Pattern	Tract of *HIS3* or *his3* sequence next to the HO site insertion
HIS3	5’ -CATATGATACATGCTCTGGCCAAGCATTCCGGCTGGTCGCT-
his3::HO	5’ -CATATGATACATGCTCTGGC--*HO*--CAAGCATTCCGGCTGGTCGCT-
A	5’ -CATATGATACATGCTCTGGC**GGTA**CATTCCGGCTGGTCGCT-
B	5’ -CATATGATACATGCTCTGGC**GGTC**CATTCCGGCTGGTCGCT-
C	5’ -CATATGATACATGCTCTGGC**GGTG**CATTCCGGCTGGTCGCT-

Extended Data Table 3

His$^+$ frequency in the *trans* and *cis* systems following transformation by HIS3.F and HIS3.R oligos

Frequency of His$^+$ transformant colonies per 10^7 viable cells for WT, *rnh1 rnh201*, and *rnh1 rnh201 spt3* mutant strains after transformation with HIS3.F and HIS3.R oligos in both *trans* and *cis* systems is shown as median and 95% CI (in parentheses). There were four or eight repeats for each of the strains transformed with these oligos. The significance of comparisons between the strains in the *trans* and the *cis* systems, and between different strains of the *trans* or *cis* system were calculated using the Mann-Whitney U test (Supplementary Table 1d). The strains used in this experiment were: YS-289, YS-290, YS-291, YS-292, YS-422, YS-423, YS-424, YS-426, YS-476, YS-477, YS-486, YS-487, HK-404, HK-407. ND, not determined.

	trans				***cis***			
Genotype	**No Oligo**		**HIS3.F + HIS3.R**		**No Oligo**		**HIS3.F + HIS3.R**	
WT	2.3	(0-8)	1.6×10^6	(1.4×10^6 -1.9×10^6)	<0.1	(0-0)	1.5×10^6	(946,000-2.3×10^6)
rnh1 rnh201	8	(0-56)	1×10^6	(1.1×10^5 -1.9×10^6)	165*	(63-275)	845,500	(669,000-1×10^6)
rnh1 rnh201 spt3	1.7	(1-2)	215,480	(196,000-235,000)	49*	(25-78)	225,300	(156,000-326,700)
rnh1 rnh201 spt3 AI Δ 23	ND		ND		<0.1	(0-0)	798,370	(610,100-1×10^6)

*We note that when the *trans* and *cis rnh1 rnh201* or *rnh1 rnh201 spt3* strains were transformed using exogenous HIS3.F and HIS3.R synthetic oligos following DSB induction, the frequencies of His$^+$ colonies were similar to each other in the *trans* and *cis rnh1 rnh201* or *rnh1 rnh201 spt3* cells. In contrast, when no oligos were added, the few His$^+$ colonies were 20 to 28-fold more numerous in *cis* than in *trans rnh1 rnh201* or *rnh1 rnh201 spt3* cells, respectively, likely originating from DSB repair by the *his3* antisense transcript.

Extended Data Table 4

His$^+$ frequencies in the presence of plasmid BDG283 or BDG606 in *cis* strains

Frequencies of Ura$^+$His$^+$ colonies per 10^7 viable cells for yeast strains of the *cis* cell system transformed with plasmid BDG283 or BDG606 following 48-h galactose or glucose treatment are shown as median and 95% CI (in parentheses). Percentage of cell survival after incubation in galactose or glucose is shown. There were 6 repeats for all the strains. The significance of comparisons between strains was calculated using the Mann-Whitney U test (Supplementary Table 1e).

Galactose

	cis		
Genotype	**Ura$^+$His$^+$ freq.**		**Survival**
WT + BDG283	36	(27-45)	9%
WT + BDG606	157,000	(143,020-193,000)	9%
rnh1 rnh201 spt3 + BDG283	820	(720-900)	25%
rnh1 rnh201 spt3 + BDG606	815	(680-900)	25%

Glucose

	cis		
Genotype	**Ura$^+$His$^+$ freq.**		**Survival**
WT + BDG283	<0.01	(0-0)	56%
WT + BDG606	<0.01	(0-0)	50%
rnh1 rnh201 spt3 + BDG283	0.28	(0.04-0.45)	93%
rnh1 rnh201 spt3 + BDG606	8	(0-24)	80%

Extended Data Table 5

His$^+$ frequencies for strains with *dbr1* null, grown in the presence of PFA, with and without the *pGAL1* promoter, grown in glucose, or containing the *AI*Δ23 intron truncation

a, Frequencies of His$^+$ colonies per 10^7 viable cells for yeast strains of the *trans* and *cis* cell system following 48-h galactose treatment are shown as median and 95% CI (in parentheses). Percentage of cell survival after incubation in galactose is also shown. 18 repeats for *dbr1* (in *trans),* 6 repeats for *dbr1* (in *cis);* 6 repeats for *rnh201 dbr1, rnh1 dbr1;* 24 repeats for *rnh1 rnh201 dbr1;* 4 repeats for PFA data. The significance of comparisons between strains was calculated using the Mann-Whitney U test (Supplementary Table 1a). **b,** Frequencies of His$^+$ colonies per 10^7 viable cells for yeast strains of the cis cell system following 48-h galactose treatment are shown as median and 95% CI (in parentheses). Percentage of cell survival after incubation in galactose is also shown. There were 6 repeats for all the strains. The significance of comparisons between strains was calculated using the Mann-Whitney U test (Supplementary Table 1f). **c,** Frequencies of His$^+$ colonies per 10^7 viable cells for the indicated yeast strains following 24-h glucose treatment in both the *trans* and the *cis* cell systems are shown as median and 95% CI (in parentheses). Percentage of cell survival after growth in glucose is also shown. There were 8 repeats for each of the strains. The significance of comparisons between the strains in the *trans* and *cis* systems was calculated using the Mann-Whitney U test (Supplementary Table 1g). ND, not determined. **d,** Frequencies of His$^+$ colonies per 10^7 viable cells for yeast strains of the *cis* cell system following 48-h galactose treatment are shown as median and 95% CI (in parentheses). Percentage of cell survival after incubation in galactose is also shown. There were 6 repeats for all the strains. The significance of comparisons between strains was calculated using the Mann-Whitney U test (Supplementary Table 1h).

a	***trans***			***cis***		
Genotype	**His$^+$ freq.**		**Survival**	**His$^+$ freq.**		**Survival**
dbr1	1,330	(1,030-1,660)	1.6%	23	(0-47)	2%
rnh201 dbr1	2,130	(1,150-3,620)	2.6%	322	(122-453)	3%
rnh1 dbr1	2,455	(1,500- 3,250)	1.2%	18	(0-78)	2.5%
rnh1 rnh201 dbr1	7,420	(7,400-11,300)	1.7%	29,900	(26,900-33,200)	1.2%
WT + PFA	519	(400-1,300)	1.7%	112	(94-380)	0.9%
rnh1 rnh201 + PFA	4,120	(3,100-5,340)	0.9%	9,400	(7,290-20,800)	0.7%

b	***cis***		
Genotype	**His$^+$ freq.**		**Survival**
WT	1,050	(600-1,460)	1%
rnh1 rnh201	62,100	(52,900-68,900)	0.7%
rnh1 rnh201 spt3	5,100	(3,660-6,660)	11%
*pGAL1*Δ	<1	(0-0)	0.4%
*rnh1 rnh201 pGAL1*Δ	540	(270-1,300)	0.4%

b	*cis*		
Genotype	**His⁺ freq.**		**Survival**
*rnh1 mh201 spt3 pGAL1*Δ	630	(500-920)	0.8%

c	*trans*			*cis*		
Genotype	**His⁺ freq.**		**Survival**	**His⁺ freq.**		**Survival**
WT	<0.01	(0-0)	16%	<0.01	(0-0)	19%
spt3	<0.01	(0-0)	96%	<0.01	(0-0)	93%
dbr1	<0.01	(0-0)	33%	<0.01	(0-0)	54%
rad52	ND		ND	<0.01	(0-0)	6%
rad51	ND		ND	<0.01	(0-0)	24%
pGAL1A	ND		ND	<0.01	(0-0)	67%
rnh1 mh201	11	(5-25)	18%	21	(17-31)	11%
rnh1 mh201 spt3	4	(2-14)	92%	9	(0.3-16)	76%
rnh1 mh201 dbr1	<0.01	(0-0)	28%	1.5	(0-6)	34%
rnh1 mh201 rad52	ND		ND	<0.01	(0-0)	23%
rnh1 mh201 rad51	ND		ND	<0.01	(0-7)	17%
*rnh1 mh201 pGAL1*Δ	ND		ND	0.9	(0-2)	45%
rnh1 mh201 spt3 rad52	ND		ND	2	(0-5)	26%
rnh1 mh201 spt3 rad51	ND		ND	2	(0-4)	50%
*rnh1 mh201 spt3 pGAL1*Δ	ND		ND	<0.01	(0-0)	85%

d	*cis*		
Genotype	**His⁺ freq.**		**Survival**
WT	1,000	(840-1,240)	2%
rnh1 mh201	43,100	(37,500-47,000)	1.7%
rnh1 mh201 spt3	4,180	(3,310-5,550)	21%
*AI*Δ23	<0.1	(0-0)	1.7%
*rnh1 mh201 AI*Δ23	<0.1	(0-0)	1.7%
*rnh1 mh201 spt3 AI*Δ23	<0.1	(0-0)	15%

Extended Data Table 6

His$^+$ rates in WT and *rnh1 rnh201* cells resulting from the transposition assay at 22 °C or 30 °C

Shown are rates of His$^+$ colonies for WT and *rnh1 rnh201* yeast strains containing BDG598 following growth with no galactose with and without plasmid selection (Ura$^-$ or YPLac, respectively) or galactose with and without plasmid selection (Ura$^-$Gal or YPLac + gal, respectively) for 96 h at 22 °C, or for 48 h at 30 °C. Data are presented as median and 95% CI (in parentheses). Percentages of cell survival after growth without or with galactose are also shown. There were 15 repeats for the strains incubated at 22 °C and 6 repeats for those incubated at 30 °C. The significance of comparisons between strains was calculated using the Mann-Whitney U test (Supplementary Table 1i). The strains used in this experiment were: TY-17, 53 and TY-22, 67.

22 °C	No gal (Ura-)		+ gal (Ura-Gal)	
Genotype	His$^+$ rate ($\times 10^{-7}$)	Survival	His$^+$ rate ($\times 10^{-3}$)	Survival
WT + BDG598	5.28 (0 – 141)	26%	2.68 (2.55 – 3.06)	15%
rnh1 rnh201 + BDG598	15.3 (16.3 – 42.4)	34%	0.78 (0.54 – 0.92)	27%
30 °C	No gal (Ura-)		+ gal (Ura-Gal)	
Genotype	His$^+$ rate ($\times 10^{-7}$)		His$^+$ rate ($\times 10^{-3}$)	
WT + BDG598	2.8 * (0 – 7.37)	26%	0.58 (0.46 – 0.72)	15%
rnh1 rnh201 + BDG598	16.1 (5.31 – 24.2)	34%	0.04 (0.03 – 0.06)	27%
30 °C	No gal (YPLac)		+ gal (YPLac + gal)	
Genotype	His$^+$ rate ($\times 10^{-7}$)		His$^+$ rate ($\times 10^{-5}$)	
WT + BDG598	<0.1 (0 – 0)	26%	1.38 (0.52 – 2.38)	15%
rnh1 rnh201 + BDG598	15.1 (4.90 – 26.4)	34%	0.4 (0.30 – 0.60)	27%

* Average.

Supplementary Material

Refer to Web version on PubMed Central for supplementary material.

Acknowledgements

We thank D. Garfinkel for plasmids pSM50, BDG606, BDG283, BDG102 and BDG598, K. D. Koh for strain KK-72, S. Y. Goo for construction of the Yep195SpGAL-*RNH201* and Yep195SpGAL-*rnh201*-D39A plasmids, S. Kowalczykowski for providing yeast Rad52 and RPA proteins, M. Fasken and A. Corbett for advices on the work and manuscript, B. Weiss, S. Balachander and C. Meers for critical reading of the manuscript, and all the people of the Storici lab for assistance and feedback on this research. We acknowledge funding from the National Science Foundation grant MCB-1021763 (to F.S.), the Georgia Research Alliance grant R9028 (to F.S.) and the National Institutes of Health CA100839 grant (to A.V.M.), for supporting this work. H.K. was supported by a fellowship from the Ministry of Science of Turkey.

References

1. Heyer WD, Ehmsen KT, Liu J. Regulation of homologous recombination in eukaryotes. Annu. Rev. Genet. 2010; 44:113–139. [PubMed: 20690856]
2. Sztuba-Solinska J, Urbanowicz A, Figlerowicz M, Bujarski JJ. RNA-RNA recombination in plant virus replication and evolution. Annu. Rev. Phytopathol. 2011; 49:415–443. [PubMed: 21529157]
3. Storici F, Bebenek K, Kunkel TA, Gordenin DA, Resnick MA. RNA-templated DNA repair. Nature. 2007; 447:338–341. [PubMed: 17429354]
4. Shen Y, et al. RNA-driven genetic changes in bacteria and in human cells. Mutation research. 2011; 717:91–98. [PubMed: 21515292]
5. Nowacki M, et al. RNA-mediated epigenetic programming of a genome-rearrangement pathway. Nature. 2008; 451:153–158. [PubMed: 18046331]
6. Derr LK, Strathern JN, Garfinkel DJ. RNA-mediated recombination in S. cerevisiae. Cell. 1991; 67:355–364. [PubMed: 1655280]
7. Moore JK, Haber JE. Capture of retrotransposon DNA at the sites of chromosomal double-strand breaks. Nature. 1996; 383:644–646. [PubMed: 8857544]
8. Teng SC, Kim B, Gabriel A. Retrotransposon reverse-transcriptase-mediated repair of chromosomal breaks. Nature. 1996; 383:641–644. [PubMed: 8857543]
9. Boeke JD, Styles CA, Fink GR. Saccharomyces cerevisiae SPT3 gene is required for transposition and transpositional recombination of chromosomal Ty elements. Mol. Cell. Biol. 1986; 6:3575–3581. [PubMed: 3025601]
10. Onozawa M, et al. Repair of DNA double-strand breaks by templated nucleotide sequence insertions derived from distant regions of the genome. Proc. Natl. Acad. Sci. USA. 2014; 111:7729–7734. [PubMed: 24821809]
11. Cerritelli SM, Crouch RJ. Ribonuclease H: the enzymes in eukaryotes. FEBS J. 2009; 276:1494–1505. [PubMed: 19228196]
12. Ruff P, Koh KD, Keskin H, Pai RB, Storici F. Aptamer-guided gene targeting in yeast and human cells. Nucleic Acids Res. 2014; 42:e61. [PubMed: 24500205]
13. Rocha PP, Chaumeil J, Skok JA. Finding the right partner in a 3D genome. Science. 2013; 342:1333–1334. [PubMed: 24337287]
14. Kohler A, Hurt E. Exporting RNA from the nucleus to the cytoplasm. Nature reviews. Mol. Cell. Biol. 2007; 8:761–773.
15. Nguyen TA, et al. Analysis of subunit assembly and function of the Saccharomyces cerevisiae RNase H2 complex. FEBS J. 2011; 278:4927–4942. [PubMed: 22004424]
16. Chapman KB, Boeke JD. Isolation and characterization of the gene encoding yeast debranching enzyme. Cell. 1991; 65:483–492. [PubMed: 1850323]
17. Karst SM, Rutz ML, Menees TM. The yeast retrotransposons Ty1 and Ty3 require the RNA Lariat debranching enzyme, Dbr1p, for efficient accumulation of reverse transcripts. Biochem. Biophys. Res. Commun. 2000; 268:112–117. [PubMed: 10652222]

18. Lee BS, Bi L, Garfinkel DJ, Bailis AM. Nucleotide excision repair/TFIIH helicases RAD3 and SSL2 inhibit short-sequence recombination and Ty1 retrotransposition by similar mechanisms. Mol. Cell. Biol. 2000; 20:2436–2445. [PubMed: 10713167]
19. Kasahara M, Clikeman JA, Bates DB, Kogoma T. RecA protein-dependent R-loop formation in vitro. Genes Devel. 2000; 14:360–365. [PubMed: 10673507]
20. Zaitsev EN, Kowalczykowski SC. A novel pairing process promoted by Escherichia coli RecA protein: inverse DNA and RNA strand exchange. Genes Devel. 2000; 14:740–749. [PubMed: 10733533]
21. Wahba L, Gore SK, Koshland D. The homologous recombination machinery modulates the formation of RNA-DNA hybrids and associated chromosome instability. eLife. 2013; 2:e00505. [PubMed: 23795288]
22. Symington LS. Role of RAD52 epistasis group genes in homologous recombination and double-strand break repair. Microbiol. Mol. Biol. Rev. 2002; 66:630–670. [PubMed: 12456786]
23. Storici F, Snipe JR, Chan GK, Gordenin DA, Resnick MA. Conservative repair of a chromosomal double-strand break by single-strand DNA through two steps of annealing. Mol.Cell. Biol. 2006; 26:7645–7657. [PubMed: 16908537]
24. Hamperl S, Cimprich KA. The contribution of co-transcriptional RNA:DNA hybrid structures to DNA damage and genome instability. DNA Repair. 2014; 19:84–94. [PubMed: 24746923]
25. Crick F. Central dogma of molecular biology. Nature. 1970; 227:561–563. [PubMed: 4913914]
26. Greider CW, Blackburn EH. Identification of a specific telomere terminal transferase activity in Tetrahymena extracts. Cell. 1985; 43:405–413. [PubMed: 3907856]
27. Crow YJ, et al. Mutations in genes encoding ribonuclease H2 subunits cause Aicardi-Goutieres syndrome and mimic congenital viral brain infection. Nat. Genet. 2006; 38:910–916. [PubMed: 16845400]
28. Curcio MJ, Garfinkel DJ. Single-step selection for Ty1 element retrotransposition. Proc. Natl. Acad. Sci. U S A. 1991; 88:936–940. [PubMed: 1846969]
29. Dombroski BA, et al. An in vivo assay for the reverse transcriptase of human retrotransposon L1 in Saccharomyces cerevisiae. Mol. Cell. Biol. 1994; 14:4485–4492. [PubMed: 7516468]
30. Stuckey S, Mukherjee K, Storici F. In vivo site-specific mutagenesis and gene collage using the delitto perfetto system in yeast Saccharomyces cerevisiae. Methods Mol. Biol. 2011; 745:173–191. [PubMed: 21660695]
31. Storici F, Resnick MA. The delitto perfetto approach to in vivo site-directed mutagenesis and chromosome rearrangements with synthetic oligonucleotides in yeast. Methods Enzymol. 2006; 409:329–345. [PubMed: 16793410]
32. Dakshinamurthy A, Nyswaner KM, Farabaugh PJ, Garfinkel DJ. BUD22 affects Ty1 retrotransposition and ribosome biogenesis in Saccharomyces cerevisiae. Genetics. 2010; 185:1193–1205. [PubMed: 20498295]
33. Storici F, et al. The flexible loop of human FEN1 endonuclease is required for flap cleavage during DNA replication and repair. EMBO J. 2002; 21:5930–5942. [PubMed: 12411510]
34. Shen Y, Storici F. Detection of RNA-templated double-strand break repair in yeast. Methods Mol. Biol. 2011; 745:193–204. [PubMed: 21660696]
35. Sherman F, Fink GR, Hicks JB. Cold Spring Harbor Laboratory Press. 1986
36. Sharon G, Burkett TJ, Garfinkel DJ. Efficient homologous recombination of Ty1 element cDNA when integration is blocked. Mol. Cell. Biol. 1994; 14:6540–6551. [PubMed: 7523854]
37. Lea DE, Coulson CA. The distribution of the numbers of mutants in bacterial populations. J. Genet. 1949; 49:264–285. [PubMed: 24536673]
38. Fasken MB, et al. Air1 zinc knuckles 4 and 5 and a conserved IWRXY motif are critical for the function and integrity of the Trf4/5-Air1/2-Mtr4 polyadenylation (TRAMP) RNA quality control complex. J. Biol. Chem. 2011; 286:37429–37445. [PubMed: 21878619]
39. Keskin H, Garriga J, Georlette D, Grana X. Complex effects of flavopiridol on the expression of primary response genes. Cell Div. 2012; 7:11. [PubMed: 22458775]

40. Sugiyama T, New JH, Kowalczykowski SC. DNA annealing by RAD52 protein is stimulated by specific interaction with the complex of replication protein A and single-stranded DNA. Proc. Natl. Acad. Sci. U S A. 1998; 95:6049–6054. [PubMed: 9600915]

41. Rossi MJ, Bugreev DV, Mazina OM, Mazin AV. Reconstituting the key steps of the DNA double-strand break repair in vitro. Methods Mol. Biol. 2011; 745:407–420. [PubMed: 21660707]

42. Sokal, RR.; Rohlf, FJ. Biometry: The Principles and Practice of Statistics in Biological Research. 2nd ed. W. H. Freeman and Company; San Francisco: 1981.

43. Storey JD, Tibshirani R. Statistical significance for genomewide studies. Proc. Natl. Acad. Sci. USA. 2003; 100:9440–9445. [PubMed: 12883005]

44. Shen Y, Koh KD, Weiss B, Storici F. Mispaired rNMPs in DNA are mutagenic and are targets of mismatch repair and RNases H. Nat. Struct. Mol. Biol. 2011; 19:98–104. [PubMed: 22139012]

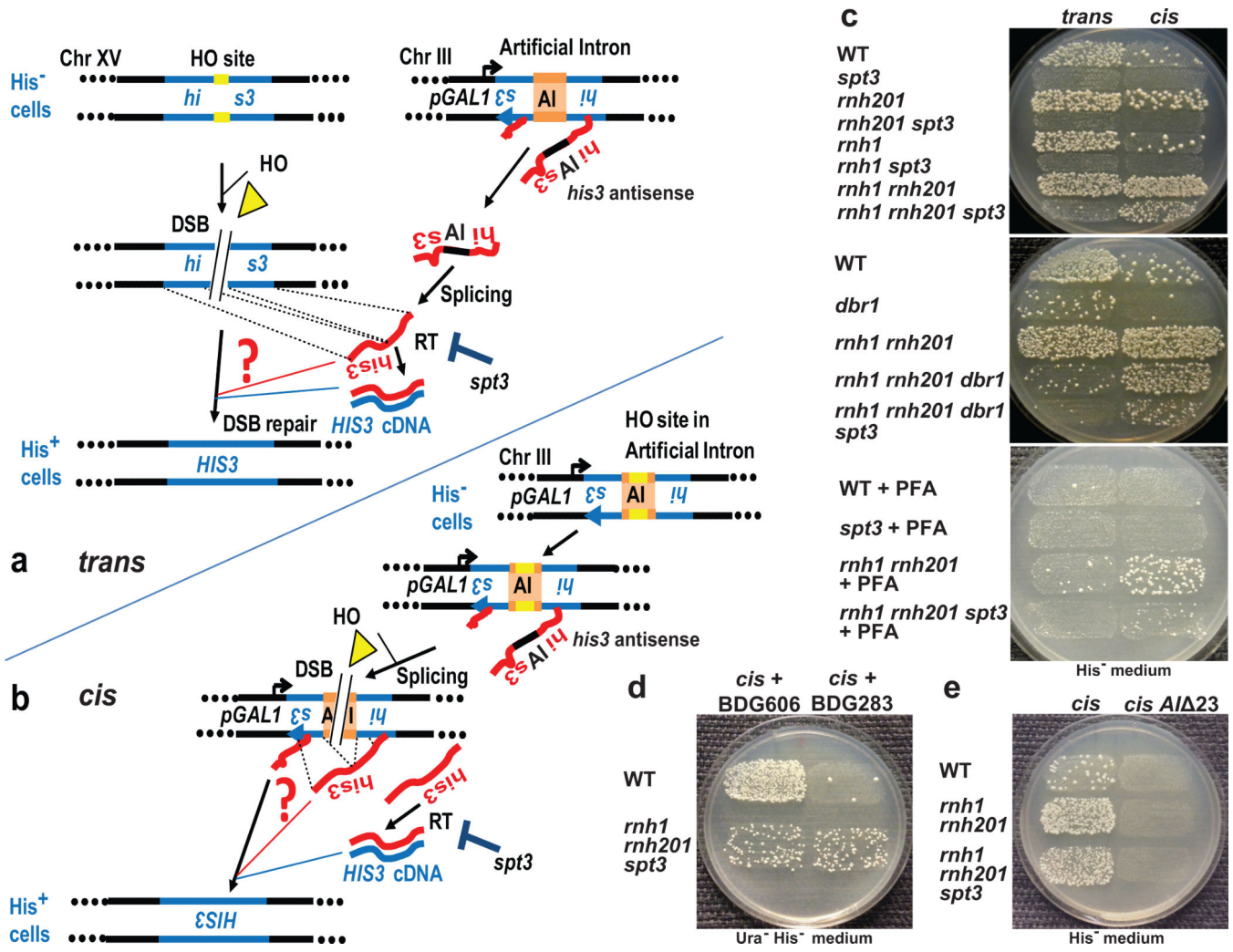

Figure 1. Repair of a chromosomal DSB by transcript RNA

Scheme of the (**a**) *trans* and (**b**) *cis* cell systems used to detect DSB repair by transcript RNA. HO, HO endonuclease; AI, artificial intron; RT, reverse transcriptase. Examples of replica-plating results (n = 6) from galactose medium to histidine dropout medium demonstrating the ability of various yeast strains (relevant genotypes shown) of the *trans* and *cis* systems to generate histidine prototrophic colonies (**c**) in the absence of *SPT3*, or *DBR1* function, or with PFA, (**d**) in the presence of the plasmid carrying the *pGAL1-mhis3AI* cassette (BDG606) or the control (BDG283), or (**e**) when the AI has a 23-bp deletion.

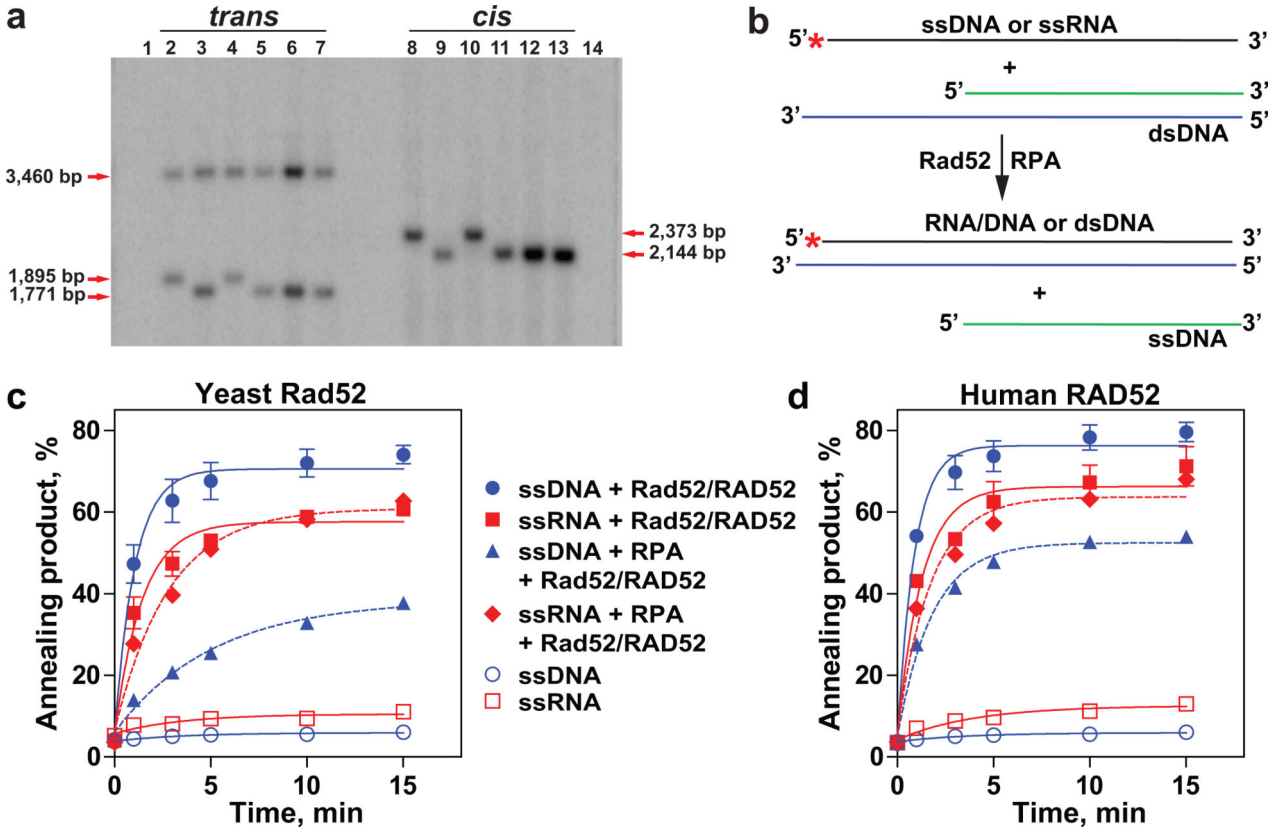

Figure 2. Transcript-templated DSB repair follows an HR mechanism

a, Southern blot analysis of yeast genomic DNA derived from *trans* WT His$^-$ (lane 2) or His$^+$ (lane 3), *rnh1 rnh201 spt3* His$^-$ (lane 4) or His$^+$ (lanes 5-7) cells, digested with BamHI restriction enzyme and hybridized with the *HIS3* probe, or derived from *cis* WT His$^-$ (lane 8) or His$^+$ (lane 9), *rnh1 rnh201 spt3* His$^-$ (lane 10) or His$^+$ (lanes 11-13) cells, digested with NarI restriction enzyme and hybridized with the *HIS3* probe (Extended Data Fig. 4a,c). Lanes 1 and 14, 1 kb DNA ladder visible in the ethidium bromide-stained gel (Extended Data Fig. 4b). Size of digested DNA bands is indicated by red arrows. **b**, Experimental scheme of Rad52-promoted annealing between RNA and DNA *in vitro*. Asterisk denotes ^{32}P label. ssDNA (#211) or ssRNA (#501) are in black, oligos #508 and #509 forming dsDNA are in blue and green, respectively. **c**, The kinetics of annealing promoted by yeast Rad52 and (**d**) human RAD52. Nucleoprotein complexes were assembled between either yeast or human Rad52 (1.35 nM) and tailed dsDNA (#508/509) (0.4 nM, molecules) in the presence (dashed lines) or absence (solid lines) of RPA (2 nM). Annealing was initiated by addition of ^{32}P-labeled ssRNA or ssDNA (0.3 nM, molecules). The kinetics of protein-free annealing reactions are indicated by open squares and circles. The error bars represent the standard error of the mean, n = 4. For the significance of comparisons between the last two time points we used the two-tailed Mann-Whitney U-test. P values are in Supplementary Table 1c.

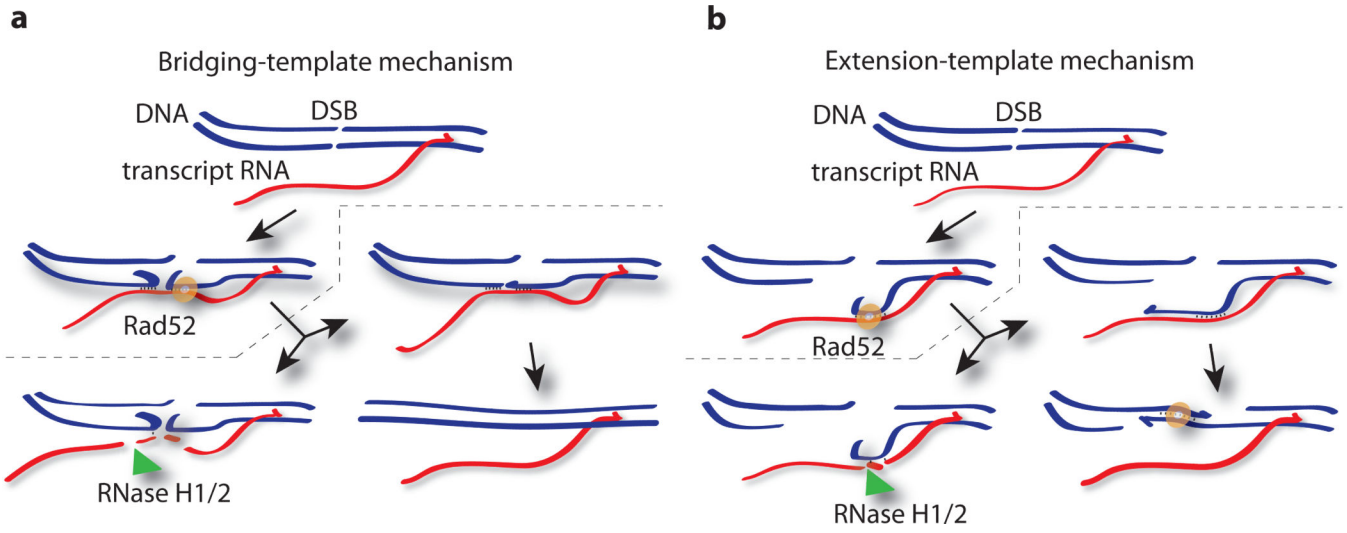

Figure 3. Models of transcript RNA-templated DSB repair in *cis*

An actively transcribed DNA region experiencing a DSB uses its own transcript RNA as a bridging (**a**) or an extension (**b**) template for repair. The small black lines indicate initial annealing between the transcript RNA and the DSB end/s, and between the two DSB ends.

Table 1

Frequencies of cDNA and transcript RNA-templated DSB repair in *trans* and in *cis*

a	***trans***			***cis***		
Genotype		**His⁺ freq.**	**Survival**		**His⁺ freq.**	**Survival**
WT	12,300	(10,000-14,600)	1.1%	2,100	(1,800-2,700)	0.7%
spt3	<0.1	(0-8)	8%*	<0.1	(0-0)	4.8%
rnh201	33,000	(30,400-42,200)	0.7%	15,800	(11,800-18,300)	0.6%
rnh201 spt3	<0.1	(0-5)	8%	<0.1	(0-0)	7%
rnh1	20,610	(17,100-23,900)	0.8%	1,780	(1,200-2,600)	0.5%
rnh1 spt3	<0.1	(0-5)	9%	<0.1	(0-10)	4.5%
rnh1 rnh201	69,000	(58,600-76,500)	1%	75,000	(57,900-82,100)	0.5%
rnh1 rnh201 spt3	642	(590-800)	11%	6,920	(5,840-7,900)	6%

b	***cis***				***cis***		
Genotype		**His⁺ freq.**	**Survival**	**Genotype**		**His⁺ freq.**	**Survival**
WT	1,640	(1,200-1,850)	1%	*rnh1 rnh201 rad51*	74,540	(55,130-87,530)	0.09%
rad52	<0.1	(0-0)	0.2%	*rnh1 rnh201 spt3*	7,560	(5,720-11,300)	7.5%
rad51	5,700	(4,170- 8,150)	0.4%	*rnh1 rnh201 spt3 rad52*	520	(300-1,100)	0.3%
rnh1 rnh201	74,600	(64,900-84,000)	0.6%	*rnh1 rnh201 spt3 rad51*	31,560	(12,910-39,220)	0.6%
rnh1 rnh201 rad52	1,520	(970-2,580)	0.1%				

a, Frequencies of His^+ colonies per 10^7 viable cells for yeast strains of the *trans* and *cis* system following 48-h galactose treatment are shown as median and 95% CI (in parentheses). Percentage of cell survival after incubation in galactose is also shown. There were 26 repeats for WT, 12 for *spt3, rnh201, rnh201 spt3, rnh1, rnh1 spt3;* 24 for *rnh1 rnh201* in both *trans* and *cis*,24 for *trans rnh1 rnh201 spt3* and 18 for *cis rnh1 rnh201 spt3.*

b, Frequencies of His^+ colonies per 10^7 viable cells for different *rad52* and *rad51* mutant strains of the *cis* system following 48-h galactose treatment are shown as median and 95% CI (in parentheses). There were 12 repeats for WT, *rnh1 rnh201 spt3, rnh1 rnh201 rad52, rnh1 rnh201 spt3 rad52, and* 6 for *rad52, rnh1 rnh201, rad51, rnh1 rnh201 rad51, rnh1 rnh201 spt3 rad51.* Percentage of cell survival after incubation in galactose is also shown. For the significance of comparisons between the strains in the *trans* and the *cis* systems, and between different strains of the *trans* or the *cis* system we used the two-tailed Mann-Whitney U test, see Supplementary Table 1a and b).

*Cells with the *spt3*-null allele have higher survival than wild-type *SPT3* cells after DSB induction because they spend more time in G2 (see Extended Data Fig. 2c).